

Institutionen för systemteknik

Department of Electrical Engineering

Examensarbete

Energy efficient, Electric-Hydraulic Power Pack

Examensarbete utfört i Elektroteknik
vid Tekniska högskolan vid Linköpings universitet
av

Johan Nyman och Amy Rankka

LiTH-ISY-EX--15/4875--SE

Linköping 2015



Linköpings universitet
TEKNISKA HÖGSKOLAN

Energy efficient, Electric-Hydraulic Power Pack

Examensarbete utfört i Elektroteknik
vid Tekniska högskolan vid Linköpings universitet
av

Johan Nyman och Amy Rankka

LiTH-ISY-EX--15/4875--SE

Handledare: **Martin Sivertsson**
ISY, Linköping University
Marcus Rösth
Hiab, Cargotec

Examinator: **Lars Eriksson**
ISY, Linköping University

Linköping, 18 juni 2015

	Avdelning, Institution Division, Department Vehicular Systems Department of Electrical Engineering SE-581 83 Linköping	Datum Date 2015-06-18
Språk Language <input type="checkbox"/> Svenska/Swedish <input checked="" type="checkbox"/> Engelska/English _____	Rapporttyp Report category <input type="checkbox"/> Licentiatavhandling <input checked="" type="checkbox"/> Examensarbete <input type="checkbox"/> C-uppsats <input type="checkbox"/> D-uppsats <input type="checkbox"/> Övrig rapport <input type="checkbox"/> _____	ISBN _____ ISRN LiTH-ISY-EX--15/4875--SE Serietitel och serienummer ISSN Title of series, numbering _____
URL för elektronisk version http://urn.kb.se/resolve?urn=urn:nbn:se:liu:diva-119477		
Titel Title Författare Authors	Energieffektivt el-hydrauliskt powerpack Energy efficient, Electric-Hydraulic Power Pack Johan Nyman och Amy Rankka Authors	
Sammanfattning Abstract <p>Along with increased oil prices and rising environmental issues, a demand for alternatives to combustion engine driven hydraulic applications has risen. In the field of mobile hydraulics, the hydraulic applications have traditionally been driven by the combustion engine of the vehicle on which they are mounted. By instead using a battery driven power pack the hydraulic application is able to operate without the engine running, saving fuel costs and reducing sound levels.</p> <p>In this thesis, the concept of using an electric-hydraulic power pack with a variable-speed electric motor and a fixed-displacement hydraulic pump to provide power to a truck-mounted loader crane is investigated. This concept is compared to an electric-hydraulic system imitating the conventional combustion engine system by using a fixed-speed electric motor connected to a variable-displacement pump. The use of a variable speed motor where the speed can be controlled electrically by a control unit creates possibilities of using different control strategies to improve the efficiency and responsiveness of the application.</p> <p>The efficiencies of the two electric-hydraulic systems are compared by constructing a physical test rig and performing measurements in a test lab. The tests have shown an increased efficiency of about 20 % when using the variable speed configuration.</p> <p>Three different control strategies are also investigated and tested on a simulated model. The simulations show that very good responsiveness and robustness can be achieved by using a hydraulic flow feed forward controller with a complementary pressure feedback controller.</p> <p>Furthermore, by controlling the hydraulic flow to the heaviest of the crane loads entirely with the flow from the hydraulic pump, the hydraulic pressure can be reduced and energy efficiency increased.</p>		
Nyckelord Keywords hybrid, hydraulic, electric, power pack, control, electro-hydraulic, loader crane		

Abstract

Along with increased oil prices and rising environmental issues, a demand for alternatives to combustion engine driven hydraulic applications has risen. In the field of mobile hydraulics, the hydraulic applications have traditionally been driven by the combustion engine of the vehicle on which they are mounted. By instead using a battery driven power pack the hydraulic application is able to operate without the engine running, saving fuel costs and reducing sound levels.

In this thesis, the concept of using an electric-hydraulic power pack with a variable-speed electric motor and a fixed-displacement hydraulic pump to provide power to a truck-mounted loader crane is investigated. This concept is compared to an electric-hydraulic system imitating the conventional combustion engine system by using a fixed-speed electric motor connected to a variable-displacement pump. The use of a variable speed motor where the speed can be controlled electrically by a control unit creates possibilities of using different control strategies to improve the efficiency and responsiveness of the application.

The efficiencies of the two electric-hydraulic systems are compared by constructing a physical test rig and performing measurements in a test lab. The tests have shown an increased efficiency of about 20 % when using the variable speed configuration.

Three different control strategies are also investigated and tested on a simulated model. The simulations show that very good responsiveness and robustness can be achieved by using a hydraulic flow feed forward controller with a complementary pressure feedback controller.

Furthermore, by controlling the hydraulic flow to the heaviest of the crane loads entirely with the flow from the hydraulic pump, the hydraulic pressure can be reduced and energy efficiency increased.

Acknowledgments

The work presented in this thesis has been carried out for Hudiksvalls Hydraulikkluster, a cooperation between several hydraulics-oriented companies of which Hiab, Sunfab and Goodtech have been involved in this project. It has been invaluable to cooperate with several companies and to have been able to take advantage of the many different skills available in different areas of interest.

We would like to thank our supervisor Marcus Rösth at Hiab for your highly valued inputs and stimulating discussions during the project. We would also like to thank Hiab, Cargotec Sweden, for providing an office and allowing us access to the facilities and equipment needed to build the test rig. A big thank you also to Pelle Gustafsson for your industrial inputs and Patric Johansson for being a great help during construction of the test rig. Also thanks to all the other guys at Hydraulics and Control systems at Hiab for sharing a great environment for questions and discussions.

We would also like to thank Sunfab for providing your well equipped test lab to carry out the hydraulic tests in. A special thank you to Jens Persson for your help during the tests as well as your thoughtful questions and feedback.

Also thanks to Goodtech and Kent Wallin for providing the control systems and helping us out with the electrical questions.

We would like to thank our supervisor at Linköping Univeristy, Martin Sivertson, for your support and feedback during the project.

Finally, a big thank you P-O Berg, project manager of Hudiksvalls Hydraulikkluster, for giving us the opportunity to carry out with this project.

*Hudiksvall, May 2015
Johan Nyman and Amy Rankka*

Contents

Notations	xi
1 Introduction	1
1.1 Background	1
1.2 Problem formulation	2
1.3 Previous work	3
1.3.1 Electric hydraulic systems	3
1.3.2 Variable-speed fixed-pump	3
1.3.3 Flow control	4
1.3.4 The approach of this project	5
1.4 Delimitations	5
1.5 Outline	5
2 Theory	7
2.1 Hydraulic systems	7
2.1.1 Constant flow system	7
2.1.2 Constant pressure system	8
2.1.3 Load sensing system	8
2.1.4 Flow control	10
2.2 Inverter	15
3 Efficiency measurements on test rig	17
3.1 Setting up the test rig	17
3.2 Performing measurements	20
4 Modeling	23
4.1 Mechanic system	25
4.2 Hydraulic system	26
4.3 Electric motor	27
4.4 Inverter	29
4.5 Battery	31
5 Control	33

5.1	Pressure feedback control	33
5.2	Flow feed forward control	34
5.2.1	Complementary pressure feedback	35
5.2.2	Adaptive parameter set	37
5.3	True flow control	41
5.4	Operator simulation	43
5.5	How to investigate the robustness of the controllers	47
5.6	Evaluation of controller performance	48
6	Results	51
6.1	Measurements on test rig	51
6.1.1	Performance during drive cycle - configuration 1	51
6.1.2	Performance during drive cycle - configuration 2	53
6.2	Controller strategy performance	57
6.2.1	Energy efficiency	58
6.2.2	Reference following	59
6.2.3	Speed	61
6.2.4	Oscillative behavior	63
6.2.5	Robustness	63
6.2.6	Performance of the adaptive parameter set	65
7	Energy study	69
7.1	Battery	69
7.2	Inverter	70
7.3	Electric motor	70
7.4	Hydraulic pump	71
7.5	Comparison	73
8	Comparison and analysis	75
8.1	Test rig	75
8.1.1	Comparison with combustion engine driven system	77
8.1.2	Environmental impact during product life-cycle	77
8.2	Simulation model	78
8.3	Simulated controllers	79
8.3.1	Energy efficiency	79
8.3.2	Discussion about speed	79
8.3.3	Discussion about robustness	79
8.4	Discussion about methods	80
9	Conclusions	81
9.1	Conclusions from this thesis	81
9.2	Future work	81
A	Selection of controllers	85
A.1	Method for selecting controllers	85
A.2	Calculation of performance factors	86

B Discussion about different types of battery packs	87
C Discussion about different types of electrical motors	91
D Cost comparison with a combustion engine driven application	95
Bibliography	97

Notations

GENERAL NOTATIONS

Notation	Meaning
P	Power
I	Current
V	Voltage
p	Hydraulic pressure
q	Hydraulic flow
ρ	Density
T	Torque

ELECTRIC NOTATIONS

Notation	Meaning
f_e	Electrical frequency
U_{oc}	Open circuit voltage of the battery
n	Rotational speed

HYDRAULIC NOTATIONS

Notation	Meaning
Δp	Difference in pressure
p_{LS}	Load sensing pressure, pressure of heaviest load
p_{pump}	Pressure after pump/system pressure
q_L	Hydraulic flow to a specific load
C_q	Flow factor, geometric parameter
A_v	Area of valve/orifice
x_v	Position of valve
$k_{g,i}$	Geometric parameter of valve
$q_{control}$	Flow signal from the controller
q_{ff}	Flow signal from the feed forward controller
q_{fb}	Flow signal from the feedback controller
q_{adjust}	Dimensionless signal from the complementary feed-back controller
q_{est}	Estimated hydraulic flow required by application
F_{ff}	Transfer function of feed forward controller
F_{fb}	Transfer function of feedback controller
η_{hm}	Hydro-mechanic efficiency of hydraulic pump
η_v	Volumetric efficiency of hydraulic pump
D_p	Displacement of hydraulic pump
ϵ_p	Variable displacement setting (=1 for fixed pumps)

1

Introduction

1.1 Background

Due to increased oil prices and rising environmental issues the need for developing more energy efficient applications is a big driving factor for development in the world today.

In mobile applications, hydraulic systems have traditionally been driven by a combustion engine connected to a hydraulic pump. This allows for great flexibility, possibility of using high power along with low cost and low extra weight, since the engine is required anyway. In recent years, falling prices of batteries and great development on customer-oriented electric vehicles, interest in using electrical motors as a power source for work hydraulics has aroused.

The proposed benefits of using an electric motor instead of a combustion engine would be lower noise levels, a lower energy cost and fewer emissions. However, a battery pack of adequate size would be expensive to purchase and be a major part of the total price of the application. An improved energy efficiency of the power pack would require a smaller battery pack, thereby significantly reducing the overall cost of the final product.

In applications where the demand for power is very uneven, the overall efficiency of an combustion engine driven system is very low, but the possible efficiency benefits of using an electric motor are very high, due to the electric motor not using any power at all during idle.

In Hudiksvall, a town with long traditions of hydraulic business, several hydraulic companies have come together and formed a "hydraulic cluster", a cooperation that focuses on education and joint projects. This master thesis project is collaborating with several of the companies in the cluster, mainly Hiab, Goodtech and Sunfab.

Hiab, a subsidiary in Cargotec, specializes in manufacturing cranes of differ-

ent sizes for mounting on on-road trucks. The cranes use a hydraulic system with cylinders and pistons for maneuvering the cranes. The power is provided by a load-sensing hydraulic pump which is connected to the diesel engine of the truck. An electric driven system could be a substitute to the diesel driven system in Hiab's applications which is why they are collaborating in this project.

1.2 Problem formulation

The purpose of this project is to study and evaluate the possibility of using a load sensing power pack featuring a *hydraulic pump with fixed displacement* where the flow is controlled by a *variable-speed electric motor* and powered by a battery (referred to as configuration 2), as opposed to an existing load sensing system with a *variable-displacement hydraulic pump* that runs on a constant speed electric motor (referred to as configuration 1). The emphasis will be on studying controllability and energy efficiency.

A model for simulation of the power-pack, the hydraulic system and the mechanical crane of configuration 2 will be produced and several control concepts will be evaluated in simulation.

A physical test rig consisting of the power pack will also be constructed and measurements will be performed on the two configurations in order to evaluate and compare energy efficiency. The test rig will be evaluated using a drive cycle similar to a general Hiab truck crane drive cycle.

The main questions to be answered during the project are:

- **Controllability:** Can the hydraulic system be well controlled by a fixed-displacement pump and a frequency-controlled electrical motor? Will the system be able to provide enough power during a specified duty cycle?
- **Efficiency:** Will the variable-speed pump with fixed displacement solution (configuration 2) be more energy efficient than a fixed-speed pump with variable displacement solution (configuration 1)? How can the efficiency of the system be increased?
- **Energy study:** How large batteries will be needed in order to provide enough energy to the system? How does the energy flow through the power pack and where is energy lost?

There are also some other interesting questions that will be briefly discussed:

- **Validity:** Will the produced model correspond well enough to the real system so that qualitative conclusions can be drawn from simulations?
- **Cost effectiveness:** Will the new solution be cost effective? Could this change in the near future due to changing prices of the components?
- **Environmental analysis:** How will the new solution affect the environment during the product life-cycle?

1.3 Previous work

In the following sections, previous work and research in different areas related to this project are discussed.

1.3.1 Electric hydraulic systems

The idea of using an electric-hydraulic power source with a load-sensing (LS) hydraulic system is not new and has been studied on several occasions, both in the industry and academia.

Berkner has written a good summary on which technologies (motors, inverters and batteries) are available on the market today and their respective pros and cons [Berkner, 2008]. The advantages of the asynchronous AC motor (that is applicable for this project) are its low cost and that it is simple to build not requiring any rare materials. The disadvantages of this motor are that it suffers from relatively poor energy efficiency and poor power density. An alternative to the asynchronous motor is the synchronous AC (permanent magnet) motor which has the advantage of higher energy efficiency but is more expensive and requires rare earth metals to be produced. Berkner further concludes that it is possible to greatly improve the energy efficiency by using an electric-hydraulic system, compared to a conventional hydraulic system.

There are also numerous studies of using hydraulic combustion engine-electric hybrids, for example Lin [Lin et al., 2009] who has studied the use of the hybrid concept in construction machine applications. Lin writes about several manufacturers that have hybrid prototypes or products. His summary states that there are large efficiencies to gain when using hybrid technology.

There are also some products available on the market based on the electric-hydraulic approach. The *Bosch-Rexroth SY.DFE* pumps for industrial use are a series consisting of a variable-displacement hydraulic pump combined with an electric motor, this configuration is proposed by the manufacturer to have the benefits of good energy efficiency and good dynamic properties.

1.3.2 Variable-speed fixed-pump

One goal with this project is to investigate whether a system with a variable-speed hydraulic pump with fixed displacement is more energy efficient than a system with a fixed-speed pump with variable displacement. This is investigated in a study by Tasner [Tasner and Lovrec, 2014] where the conclusion is that the latter system is the more energy efficient. The drive cycle used in the study differs from the cycle planned to be used in this project in the fact that it does not include any idle parts. The ability to slow down the speed of the motor to zero when idling is a big benefit with the prior system and the answer to which system is most energy efficient doesn't have to be the same in this project. Tasner's results indicate however that the difference in efficiency might not be very big. Tasner also studies a third concept, which is a combination of the two mentioned above, with a pump with both variable speed and variable displacement. This gives an

additional degree of freedom and as a consequence a possible higher efficiency than the two other systems but also requires a more complicated controller. The study presents such a controller but the possibility of using it is outside the scope of this project.

Lovrec et al [Lovrec et al., 2008] has also studied the concept of using a system with a fixed displacement pump and an induction motor with variable speed for usage in an industrial forming machine. This is the same motor-pump configuration as in this project, the results from the study is therefore a good indicator of the challenges and expectations of this project. Lovrec et al conclude that there are some issues in responsiveness due to the high inertia of the electric motor compared to the inertia of a variable displacement pump, although there are improvements gained in the overall efficiency compared to an ordinary LS system.

Minav [Minav et al., 2012] has conducted a study of using the hydraulic pump, directly driven by an electric motor, to power a lifting system. The pump has a fixed displacement and the hydraulic flow is controlled by varying the speed of the motor (as is the case this project). Minav discusses the possibility of recuperation during lowering of the load, however in this project this opportunity will not be considered due to the need of modifying the hydraulic system. In general, by using an electric motor the energy efficiency increased, even when not considering recuperation.

1.3.3 Flow control

In this project the concept of controlling the flow directly from the pump, so called "flow control", will be used. The main difference between flow control and traditional load sensing (LS) systems is that the flow is directly controlled (fed forward) from an operator "required flow" signal, unlike the load sensing system which utilizes a pressure feed-back loop in order to control the flow.

Eriksson [Eriksson, 2010] has studied the difference between a flow controlled system and a conventional LS-system on a drive cycle for a wheel loader. The result from the study is that the energy consumption of the flow controlled system is about 14 % lower than that of the LS-system (for that specific application). The flow controlled system is also found to be less oscillative than the LS-system.

Axin et al [Axin et al., 2014] have conducted a study of the flow control concept on a wheel loader application. The increased stability of the feed forward control compared to an LS system is discussed and found to be in great favor to the flow control concept. The reason for this is that the responsiveness of a (LS) feed-back loop is often limited by stability issues in the stiff hydraulic system, whereas the feed forward flow controller can be designed considering only the desired properties of the system, without having to take stability issues into account. Axin et al also conclude that there are reduced energy losses in the system due to lower pressure drops over various components when using flow control, rendering a better overall energy efficiency.

The company Parker is promoting a flow controlled hydraulic system [Stegemann and Acharya, 2011], claiming great benefits in terms of efficiency and performance in comparison to traditional (such as constant pressure, constant flow

and load sensing) hydraulic systems.

1.3.4 The approach of this project

The approach of this project is to try to increase the overall efficiency of an LS-designed hydraulic system by using the flow control concept, together with a fixed displacement pump and a variable speed motor. This specific configuration has not been found by the authors to have been studied before. This is probably due to that a more conventional approach for using the flow control concept has been to initially design the hydraulic system with regards to flow control, rather than using an unmodified LS-designed hydraulic system.

By specifically *not* modifying the hydraulic system, other than the pump, this control concept is possible to apply on a modular or an already existing system.

Although this specific configuration may not have been studied before, the results mentioned earlier indicate that it might be a good solution with regards to energy efficiency and controllability.

1.4 Delimitations

Hydraulic system design: The hydraulic system (not specifically considered to be a part of the power pack) is not modified. This means that the system's using valves designed for a traditional load sensing hydraulic system.

Selection of components: The hydraulic pump is selected from the Sunfab product series. The induction motor that was already installed on the test bench is not replaced, but the possibility of using a smaller motor or a permanent magnet motor is discussed.

Testing and comparison of the systems: The systems are not compared with regards to the ability to withstand rough conditions, such as extreme temperatures, altitude or other uncommon usage environments.

Energy study of the power pack: The efficiency is only calculated for the battery, the motor and the pump. It is not investigated in detail which parts in the above components that give rise to the energy losses.

1.5 Outline

This report is made up of nine chapters, this one being the first. The theory behind the concepts and components used in the project and present in the report is presented in the second chapter. The theory lays the base of understanding needed to carry out a thesis project in the area for a reader with an engineering background.

The third chapter describes the work of constructing the test rig with the two different configurations to be compared and how efficiency measurements were carried out.

Chapters four and five concern the simulation model of the system with a fixed displacement pump. The fourth chapter describes the different parts of the

model, how they are implemented and how they are validated in the cases where validation is possible. In the fifth chapter the structures of the different control strategies are presented, as well as their implementations in the simulation model.

The results from the measurements on the test rig and the simulations of the model are presented in chapter six. The results from the measurements focus on energy efficiency and the results from the simulations focus on controller performance.

The seventh chapter is a study of the energy flow through the different components of the power pack. The study is carried out on the simulation model but the results are applied to the physical components of the system. The chapter also includes discussions about how well the components are matched to the typical operation of the system with regards to efficiency.

In chapter eight a comparison of the two configurations of the system on the test rig is presented and discussed. A comparison is also made and discussed between the different control strategies implemented in the model. The pros and the cons of using an electric system are discussed.

Finally, the conclusions of the thesis are presented in the last chapter together with recommendations on interesting future work based on the results of this thesis.

2

Theory

2.1 Hydraulic systems

The biggest advantage of a hydraulic system compared to an electrical power system is that the hydraulic actuators (i.e. motors, pistons etc) have a very high power density, which makes them much more attractive to use in mobile systems where a high amount of power is required as well as a low weight.

There are several kinds of hydraulic systems, which differ in terms of how the pressure and flow of the hydraulic fluid is created and controlled.

2.1.1 Constant flow system

The most basic kind of hydraulic system is the constant flow system, where a pump is running continuously, providing a constant hydraulic flow to the system. The loads (i.e. motors, cylinders etc) are controlled by valves of *open-center* type (see Figure 2.1), which means that when the valve is in idle (center position) the flow passes right through the valve and to the next one (or the tank, in the end). This means that when the whole system is idle, the hydraulic flow runs straight from the pump, through each valve and back to the tank. When a valve is shifted from the idle position, the flow is diverted to the load in question, and the pressure in the system (which in idle is low) will rise to meet that of the load.

This kind of system is simple, due to the simple components required, but unfortunately very energy inefficient, especially when idle or at low speeds (i. e. low flows), see Figure 2.2. Another drawback is that the velocity of different loads will be dependent of each other, since they share a common path of the hydraulic flow.

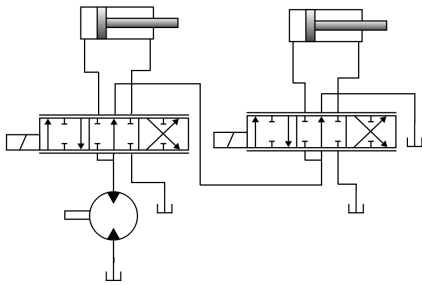


Figure 2.1: Schematic of a simplified constant flow system. The loads are connected in series with the hydraulic pump.

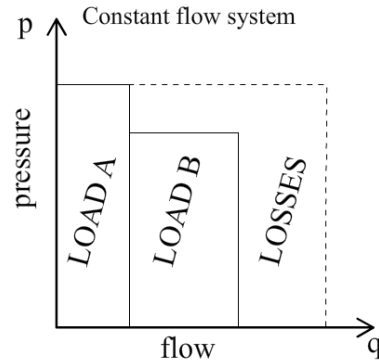


Figure 2.2: pq -diagram of a constant flow system. The "losses"-area represents power lost due to excess flow from the hydraulic pump.

2.1.2 Constant pressure system

Another kind of system is the constant pressure system, see Figure 2.3, where the hydraulic pressure is kept constant by a variable displacement pump¹. The loads are controlled by valves connected to a common pressure rail. Since the pressures to the loads will be kept constant by the pump, the functionality of different loads won't be dependent of each other.

This kind of system uses less power than the constant-flow system when idle, but still suffers from poor energy efficiency when moving light loads, see Figure 2.4.

2.1.3 Load sensing system

A load sensing system, *LS-system*, features a variable-displacement pump that keeps the system pressure at a certain level, Δp , above the pressure determined by the heaviest load.

The pump receives the maximum load pressure, the LS-signal, through a series of check-valves from the loads, see Figure 2.5. Since the system pressure is determined by the heaviest load, this kind of system is very energy efficient when moving a single load, but when moving multiple loads there might be significant losses, see Figure 2.6, due to pressure drops in the valves controlling the flows to lighter loads.

Since the system pressure varies, the flow through a valve is not only dependent of the valve position but also of other loads. Since it is desirable to have the flow dependent only of the valve position, a *compensator valve* is inserted at each valve, which keeps the pressure drop over the valve constant at a certain level.

¹A variable displacement pump features a mechanism for adjusting its displacement (i. e. volume output per revolution), often controlled by a hydraulic pressure.

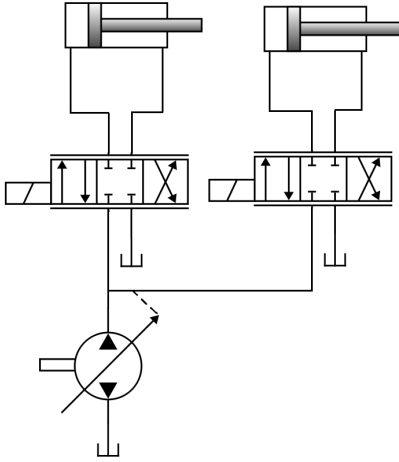


Figure 2.3: Schematic of a simplified constant pressure system. The loads are connected in parallel to a common pressure rail, rendering the functionality of the loads independent of each other.

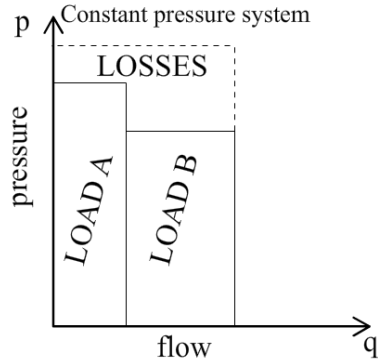


Figure 2.4: pq -diagram of a constant pressure system. The "losses"-area represents power lost due to excess pressure from the hydraulic pump.

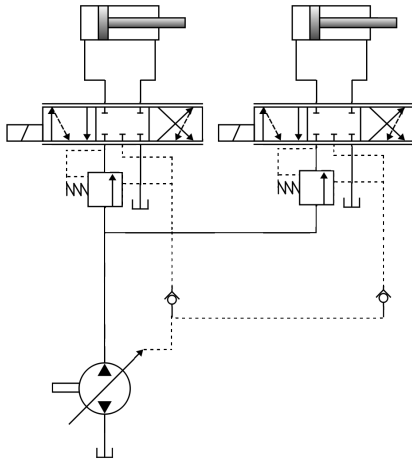


Figure 2.5: Simplified schematic of a load sensing hydraulic system. The loads are connected in parallel to a common pressure rail, where the hydraulic pump uses the pressure of the heaviest load to control the system pressure.

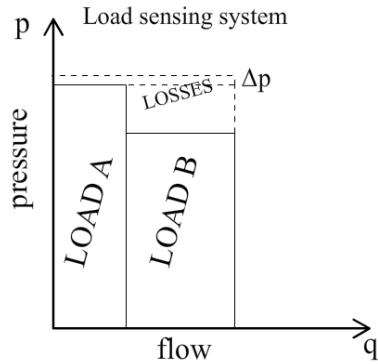


Figure 2.6: pq -diagram of a load sensing hydraulic system. The losses are smaller compared to previous systems, but can still be significant if the pressures of different loads differ.

The flow through the valve and to the load, q_L , is determined by the following equation:

$$q_L = C_q A_v \sqrt{\frac{2}{\rho} (p_1 - p_2)} \quad (2.1)$$

where the opening area $A_v = A_v(x_v)$ is dependent of the valve position x_v . Since the pressure drop over the valve, $p_1 - p_2$, is kept constant, the flow will only be dependent of the valve position.

2.1.4 Flow control

In a hydraulic application, it may be desired by the operator to control the speed of a movement by the angle of a joystick. In this case the hydraulic flow required from the pump can be determined by measuring the joystick positions and calculate an estimated required flow, see equation 2.2.

$$q_{est} = \sum_{i=0}^n f(x_i) k_{g,i} \quad (2.2)$$

The function $f(x)$ is an arbitrary, possibly nonlinear function often designed to increase the sensitivity of small movements and fine adjustments. The $k_{g,i}$ are geometric parameters derived from the valve and load characteristics and n is the number of functions.

The hydraulic system which diverts the hydraulic flows can be almost identical to the LS-system, with the exceptions that the flow from the hydraulic pump will now be controlled by a controller and the LS-pressure is measured by a sensor.

When the operator requests a certain movement of a load, the required flow of the system will be fed-forward to control the speed of the hydraulic pump, along with a signal to the directional valve in question to be opened. As the flow from the pump increases, the pressure at the pump will also increase until it is higher than that of the load, which will cause a flow to the load through the valve.

The biggest advantage of using a feed-forward concept to control the speed of the pump is that the stability of the system will improve. Hydraulic systems are generally quite under damped and by controlling the systems with a feedback loop (such as the previously discussed pressure controlled LS system) large oscillations can easily occur if the controller is not tuned correctly, or dampened further by adding hydraulic dampeners. By using a feed-forward loop instead, the risks of oscillations are significantly reduced and the speed of the controller can be increased without much risk of instability.

Pressure feed-back

As with all feed-forward controllers, the performance of the controller could be largely affected by errors in the model estimation (in this case; the required hydraulic flow estimation).

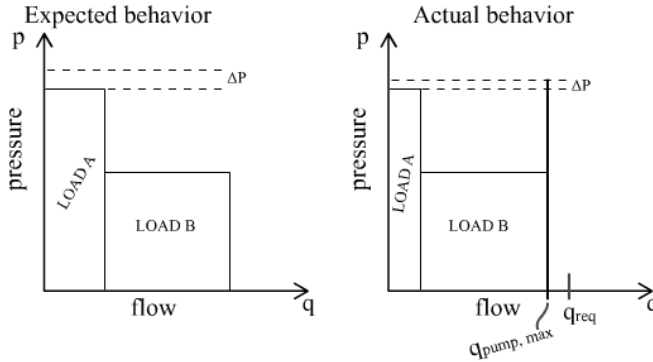


Figure 2.7: Left: The desired flow and pressure of two loads. Right: The actual flow and pressure of the loads, the flow to Load A is reduced due to pump saturation.

An error in the model will result in a too high or a too low flow from the hydraulic pump. These two situations are discussed below:

- **The controlled flow from the feed-forward controller is too low.**

This could be due to that the pump flow is saturated, or that there is a model error in the feed-forward controller.

When the flow is too low the compensator valve of the heaviest load will react by opening fully, but the flow to the load will still be lower than expected, or even none at all.

Due to the lower flow, the pressure drop over the compensator valve, Δp , will be lower than usual, see figure 2.7

- **The controlled flow from the feed-forward controller is too high.**

This is probably due to a modeling error in the feed-forward controller.

When the flow is too high the compensator valves of the different loads will close and only allow their share of flow through them. The pressure at the pump will rise until the pressure relief valve opens up, essentially creating a constant pressure system with great power losses, see Figure 2.8.

In order to cope with the errors in the feed-forward controller model, effectively causing unwanted pressure variations, a feedback controller is introduced to compensate for these behaviors.

The resulting controller will achieve an initial fast response (thanks to the feed forward controller) and, in a short while, a correct flow and pressure level thanks to the feed-back controller.

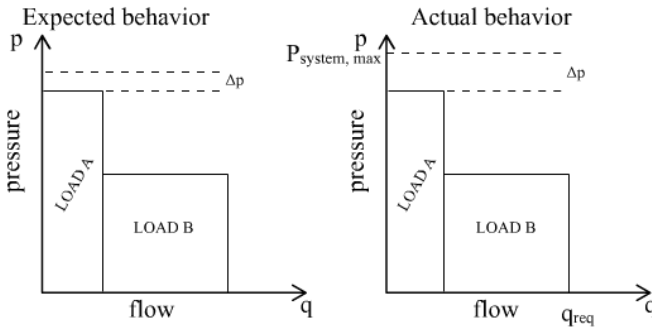


Figure 2.8: Left: The desired flow and pressure of two loads. Right: The actual flow and pressure of the loads. The pressure rises to max system pressure due to a too high flow from the pump.

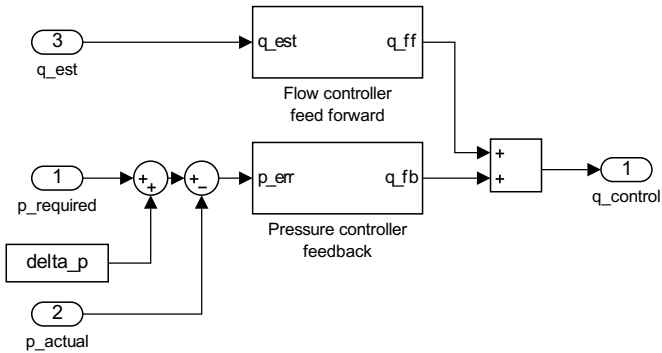


Figure 2.9: Overview of the feed-forward control strategy. The resulting control signal is the sum of the signals from the feed forward and the feedback control blocks.

Adaptive parameter set

As previously discussed, the feed forward controller uses the control signal q_{est} that can be calculated from the sum of the operators signals together with the geometric parameters $k_{g,i}$.

An error in the geometric parameters would result in an error in the calculated required flow, making the performance of the feed-forward controller worse. Unfortunately, the geometric parameters may be hard to determine exact, due to manufacturing variations, operating conditions or wear. If the exact flow to each of the loads could be measured the relation between the operator signals and the resulting flows would be known and the current values of the parameters determined. Flow-measurement sensors are however quite expensive and/or inaccurate so another approach with a quasi-observer that estimates the parameters is proposed:

When using a feed-forward controller together with a feed-back controller, the feed-back controller should ideally be outputting a value not modifying the feed forward signal at all, and an ideal feed-forward controller should take care of all control signals needed to control the system.

However, when introducing a model error in the feed-forward controller the feed-back controller will take care of the adjusting needed in order to cope with the model error.

A schematic view of the controller can be viewed in Figure 2.9. A correlation between the estimation error of the feed forward controller, $q_{est,err}$, and the feedback control signal, q_{fb} , can be derived using Equations 2.3 through 2.9.

The feed forward flow signal is a function of the estimated flow (see Equation 2.2).

$$q_{ff} = F_{ff} q_{est} \quad (2.3)$$

The total flow signal is the sum of the feed forward and the feedback flow signals.

$$q_{control} = q_{ff} + q_{fb} \quad (2.4)$$

The estimation error of the flow is the difference between the actual flow and the estimated flow.

$$q_{est,err} = q_{actual} - q_{est} \quad (2.5)$$

The system flow error is the difference between the control signal (sent to the inverter) and the actual flow (coming from the pump).

$$q_{sys,err} = q_{actual} - q_{control} = (q_{est,err} + q_{est}) - (F_{ff} q_{est} + q_{fb}) \quad (2.6)$$

\Leftrightarrow

$$q_{fb} = q_{est} + q_{est,err} - F_{ff} q_{est} - q_{sys,err} \quad (2.7)$$

When looking at steady state, the system flow error can be assumed to reach zero and the feed forward controller to reach one.

$$t \rightarrow \infty \Rightarrow q_{sys,err} \rightarrow 0, F_{ff} \rightarrow 1 \quad (2.8)$$

In time, the feedback controller signal q_{fb} will thus approach the estimation error in flow, $q_{est,err}$.

$$t \rightarrow \infty \Rightarrow q_{fb} \rightarrow q_{est,err} \quad (2.9)$$

This implies that the q_{fb} signal could be used as a measure of the estimation error.

The weighted values, N_i are introduced as a way of determining which of the parameters $k_{g,i}$ that are currently affecting the model estimation:

$$N_i = \int_{t=t_0}^{t_1} f(x_i) dt \quad (2.10)$$

$$N_{n,i} = \frac{N_i}{\sum_{i=1}^m N_i} \quad (2.11)$$

$N_{n,i}$ are normalized values between (0-1).

Thanks to the linear relation between $k_{g,i}$ and q_{est} in equation 2.2 it is easy to realize that the model error q_{err} will be counteracted by increasing/decreasing the current acting $k_{g,i}$ according to equation 2.12.

$$\dot{k}_{g,i} = N_{n,i} k_{g,i} q_{err} K_{obs} \quad (2.12)$$

K_{obs} is a design constant, determining the rate of changes in $k_{g,i}$. K_{obs} is typically selected so that the value of $k_{g,i}$ reflects the average value from a large number of previous movements.

True flow control

In Section 2.1.4 the situation that arises when the hydraulic flow from the pump is lower than required by the constant-flow valves is discussed. A side effect can be seen in Figure 2.7, more precisely the slightly lower Δp that occur due to the constant-flow valve opening fully (since it is trying to keep the flow constant) and thereby lowering the pressure loss over the valve.

By forcing the valve of the heaviest load (the one that requires the most pressure) to open fully the flow through the valve will instead be controlled by the speed of hydraulic pump. The fully opened valve will cause a lower pressure drop, thus reducing the pressure of the whole hydraulic system resulting in increased energy efficiency.

This control concept is referred to as "True flow control" in this thesis, however variations of this concept have been studied before and it is known simply as "Flow control".

2.2 Inverter

The purpose of an inverter, or a variable frequency drive, is to output AC current at variable frequency. The amplitude and frequency of the current then determine the speed of the electric motor. Three different control strategies for controlling the frequency of an induction motor are common today, scalar control in the form of constant voltage-frequency control (V/Hz), or vector control in the form of field-oriented control (FOC) or direct torque control (DTC). FOC and V/Hz are used in this project and will be further explained in this section.

The idea of FOC is to control the torque and the rotor flux independently of one another in order to achieve a fast response to changes in operating conditions. This is possible by using the so called dq0 transformation to transfer the stator flux and current into two components each that rotate synchronously with the rotor.

The principle of the V/Hz control is to keep a constant magnetic flux density and thereby a constant maximum torque in the motor for frequencies equal to or lower than rated. If only the frequency was changed to change the speed of the motor the flux would be so high at low frequencies that the motor could be damaged due to large core losses and large currents. If the input voltage V_a is changed along with the electrical frequency f_e to satisfy Equation 2.13 then the flux remains constant if the voltage drop over the stator resistance is neglected.

$$\frac{V_a}{f_e} = \frac{V_{a,rated}}{f_{e,rated}} \quad (2.13)$$

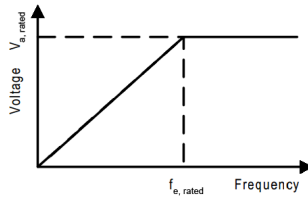


Figure 2.10: Relation between voltage and frequency during constant V/Hz control. The ratio of voltage to frequency is constant up to a maximum voltage level.

Since the voltage should not be higher than rated to avoid damage on the insulation of the motor it is kept at its rated value as the frequency increases over the rated frequency, see Figure 2.10. In this region, the magnetic flux is no longer constant and the maximum torque decreases since it is now proportional to the inverse of the frequency. Instead of the torque, the maximum power is now kept constant according to Equation 2.14 since the voltage is equal to V_{rated} and the current is independent of the frequency and allowed to take the values up to I_{rated} .

$$P_{max} = V_{rated} I_{rated} \quad (2.14)$$

3

Efficiency measurements on test rig

In order to measure and evaluate the concept of using a variable-speed controlled hydraulic pump, compared to a conventional fixed-speed variable-displacement pump, a test rig is built in order to perform tests and gather measurements of the two system configurations.

3.1 Setting up the test rig

The test rig (see Figure 3.1) is based upon an existing rig that has been used by Hiab to evaluate an electric-hydraulic drive with a fixed speed motor and a variable displacement pump in a previous project.

Several components are reused from the old rig. The old frame, oil tank, electric motor, battery and variable pump are all kept, whereas the old inverter is replaced with a newer one which features better controllability. Discussions about how to select a suitable battery or electric motor can be found in Appendix B and C, if a replacement of those components would be relevant in the future.

The components of the test rig and their connections to one another are displayed in Figure 3.2. The properties of the components are described below.

Battery

The battery is a conventional lead-acid battery at 40kWh with a peak voltage of 120 V if all cells are connected. For the tests of this project the voltage is limited to 94 V in order not to overload the inverter.

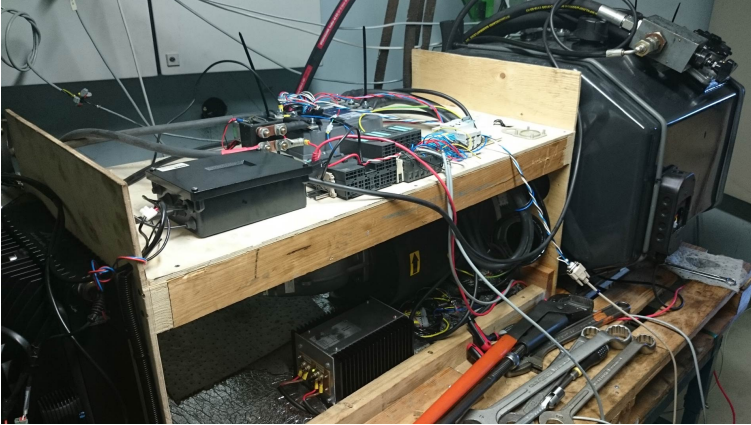


Figure 3.1: The test rig. The electric motor and hydraulic pump are located at the lower level. At the top the inverter and controller PLC are located. The hydraulic tank is in the back.

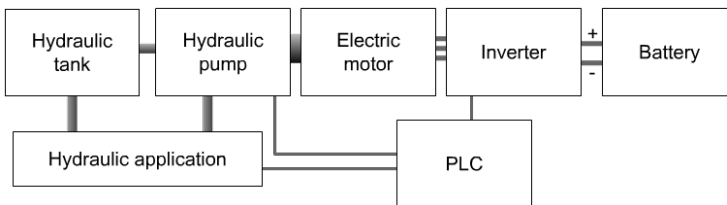


Figure 3.2: Schematic overview of the test rig.

Electric motor

The motor is of asynchronous type with nominal data according to Table 3.1. It is reused from the old rig and not selected specifically for this project. The efficiency of the motor as a function of speed and torque can be viewed in Figure 3.3.

Voltage	80 V
Power	47 kW
Current	418 A
Speed	2339 rpm
Frequency	80 Hz

Table 3.1: Nominal data of the electric motor.

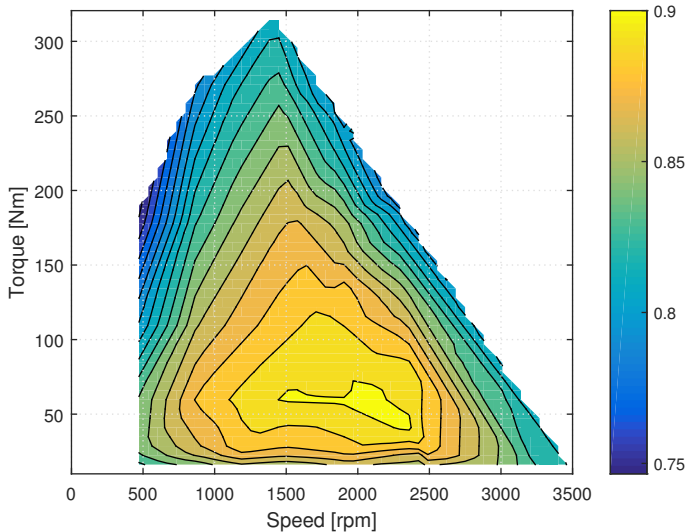


Figure 3.3: Efficiency map of the motor, derived from measurement data from the motor manufacturer.

Inverter

The inverter is rated at 24.5kVA at continuous operation with a current limit of 550 A and a nominal voltage of 80 V. It uses the Field-Oriented Control (FOC) strategy explained in Section 2.2 and receives a reference speed signal from the PLC to control the speed of the motor.

The inverter has many features such as signal filtering, speed ramps etc that could be useful in other types of applications. In this project however, it is desired

to have a step response that is as quick as possible, thus most of the filtering options are subsequently turned off or set to as quick as possible.

PLC - controller

The PLC is a programmable logic controller responsible for controlling things such as:

- Turning power on and off, based on key switch or emergency kill switch.
- Receive measured pressures from pressure sensors.
- Calculate desired motor speed.
- Sending reference speed signal to the inverter.

The control strategy used on the test rig is a pressure feedback control and it calculates the speed required by the motor to maintain the correct pressure in the hydraulic system by reading measurements of the pump pressure and the LS-pressure from the hydraulic test equipment, see Section 3.2. The control strategy is developed in Simulink and then implemented in the PLC.

3.2 Performing measurements

The test rig is tested in a hydraulic lab where a test cycle with predefined flows and pressures can be applied to the test rig. The pressures and flows of individual functions cannot be simulated, making pressure feedback control the only available strategy of the control strategies proposed in Chapter 5.

The reasons for using a predefined load cycle instead of a real hydraulic crane are lower costs, better repeatability and easier logistics.

The original drive cycle, see the left part of Figure 3.4, is derived from several operating points given by a crane simulator, where the crane performs a typical "lift and move" operation. The pressures and flows between the points are linearly interpolated in order to be able to create the cycle with simple ramps and steps.

When the test rig was initially tested it became clear that it would not be able to reach some of the toughest operating points in the drive cycle, due to a lower maximum power output than previously expected. The culprit to this is mainly a voltage drop from the battery in combination with the inverter.

Since there was no available way of increasing the power output an easier drive cycle is used instead, with lower flows and lower pressures, see the right part of Figure 3.4. Compared to the original cycle the flows and pressures have been decreased and the cycle time has been increased, rendering a lower maximum power needed. Since the pressure over the pump and the pump torque are closely related, the decreased pressure effectively reduces the torque required of the motor to complete the drive cycle.

Another change is that the flow is saturated to a lower level of 10 litres/min since the hydraulic lab equipment cannot keep a lower flow than that constant.

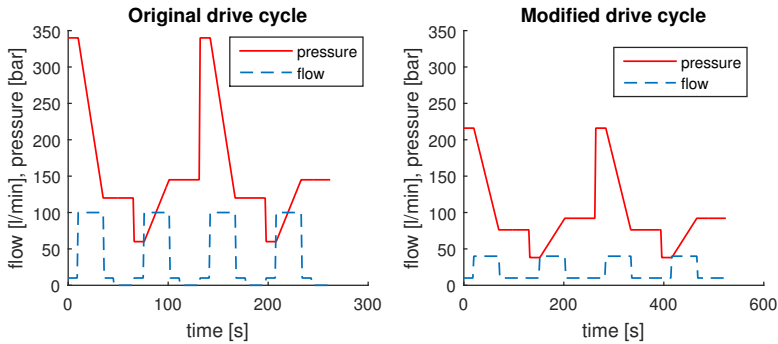


Figure 3.4: Original (left) and modified (right) drive cycles with flow and pressure levels. The modified drive cycle features lower pressure and flows but has a longer duration.

Although this is not ideal, the results in the following tests are considered to be scalable to reflect the original drive cycle, if considering the following things:

- The motor is rated at 47kW, thus is currently under loaded. A somewhat lower efficiency can be expected when putting on lighter loads.
- The battery is operating at its maximum power output and needs to be replaced with a bigger one to be able to increase overall power output. Increasing the battery size will also have a positive effect on battery efficiency during discharge thanks to a lower internal resistance.

Measurements were performed on the two different configurations of the test rig:

- Configuration 1: Fixed speed motor and variable displacement pump
- Configuration 2: Variable speed motor and fixed displacement pump

During the tests, the following signals are measured:

- Battery voltage, transformed from 0-100 V to 0-10 V
- Battery current, 0-400 A transformed to 0-400 mV
- Pump pressure, measured as 4-20 mA
- LS-pressure, measured as 4-20 mA
- Pump flow

The signals are connected to a LabView [Lab] based interface where they can be monitored and logged, the following *drive cycle tests* were performed:

- Drive cycle test with configuration 1 - pump with variable displacement, speed of motor fixed to 2000 rpm

- Drive cycle test with configuration 1 - pump with variable displacement, speed of motor fixed to 2500 rpm
- Drive cycle test with configuration 2 - pump with fixed displacement, variable motor speed, two test runs

4

Modeling

In order to be able to construct satisfactory control strategies, a model of the full application is built in MATLAB Simulink.

The model is constructed with the following constraints in mind:

- The model should capture dynamic behaviors from the mechanic system (the crane) in order to present variations in hydraulic pressures depending of load, crane position, speed and acceleration.
- The model should capture dynamic behaviors from the hydraulic system in order to provide some of the behaviors of a load-sensing hydraulic application as well as the challenges in controlling it.
- The model should capture dynamic behaviors down to approximately 0.1 seconds in order to provide a suitable subject for the controllers.
- The efficiencies of the different components should be modeled, to enable analysis of energy flow through the system.

The model of the system consists of several component models, a battery, an inverter (a variable frequency drive), an electric motor, a rotating mass, a hydraulic system and a mechanic system. The model, made up of the component models and the signals connecting them, can be viewed in Figure 4.1. The controller structure (seen as the "Controller" block in the figure) is largely neglected in this chapter and is described later on.

As seen in Figure 4.1, most of the blocks have one or more input-output pairs of signals, for example the battery has an input of electric current and an output of voltage. To determine which of these signals are to be inputs or outputs, a *bond graph* is constructed and causalities are determined. For example it can be seen by looking at the battery junction in the bond graph, see Figure 4.2, that the causality mark of the arrow connected to the inverter is pointed outwards,

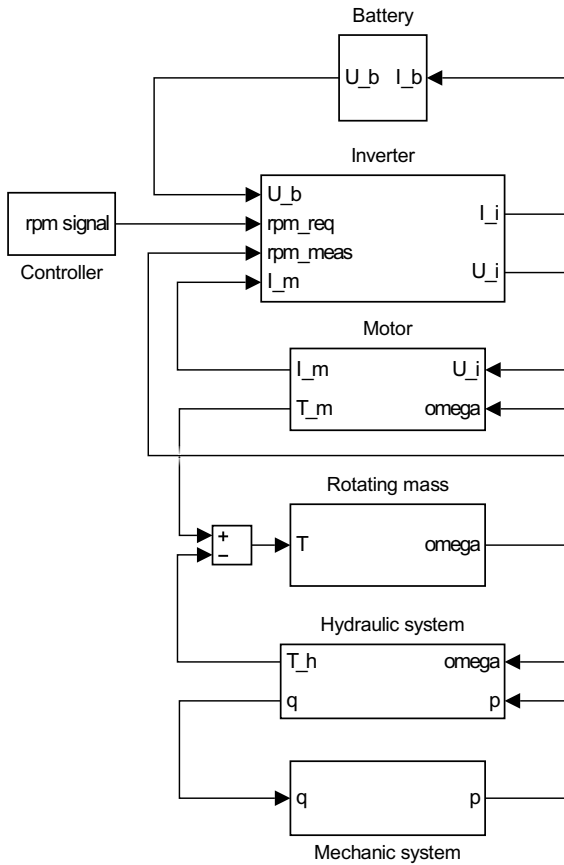


Figure 4.1: A simplified overview of the Simulink model. The different subsystems are connected in series and the power flows from the battery, through the whole system and finally into the mechanic system.

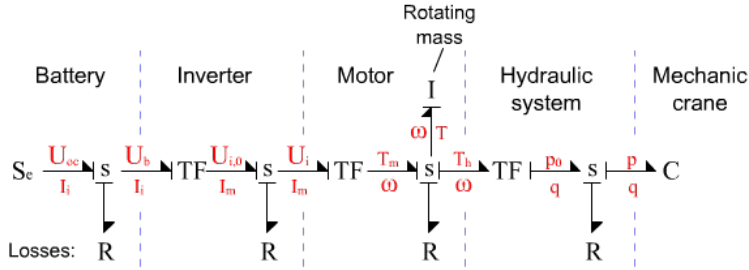


Figure 4.2: Bond graph of the model. The power flows through the system from left to right.

towards the inverter. This implies that the effort variable (the voltage) is to be modeled as an output and the flow variable (the electric current) as an input.

In the bond graph, see Figure 4.2, it can also be noted that most of the components work as transformers, transforming power between physical domains (e.g. the motor transforms electrical power to mechanical power, the hydraulic pump transforms the mechanical power to hydraulic power) or transforms power within the same domain (e.g. the inverter converts electrical power to another electrical power).

The rotating mass of the motor and pump is the only inductance in the system, thus is determining the flow variables (i. e. current, angular velocity and hydraulic flow) of the system. The mechanic system is considered a capacitance, determining the effort variables (i. e. voltage, torque and pressure).

4.1 Mechanic system

The mechanic model is a simplified model of one of Hiab's hydraulic cranes, modeled in SimMechanics and provided by Hiab. The appearance of the model crane can be seen Figure 4.3. The mechanic model features several motions of the crane as well as a linkage system for the cylinders. There are four ways of moving the crane in this model: Rotating the crane at the base, lifting the first boom with cylinder A, lifting the second boom with cylinder B and extending the crane. The function rotating the crane at the base will not be actively used in this project since it has proven too hard to control by the operator simulator, see Section 5.4. There are also linkage systems that connect the cylinders with the next boom. The linkages are geometrically designed so that the effective lever distance between the cylinders and the rotation point is more advantageous at different angles than what would otherwise be possible.

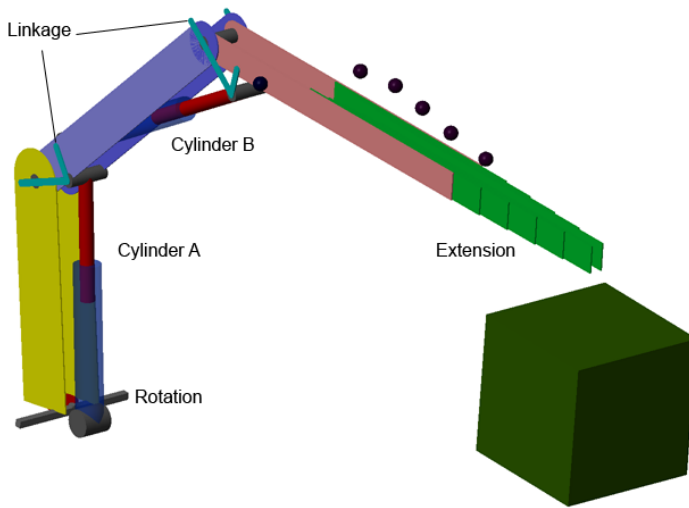


Figure 4.3: 3D model of the crane, with its different components marked in the figure.

The mechanic model receives hydraulic flows to its four functions. The flows cause pressures to build up inside the cylinders, which in turn causes the crane to move. The built up pressures are fed back to the hydraulic system.

4.2 Hydraulic system

The hydraulic system is a simplified model derived from Hiab's load-sensing hydraulic valves. To accurately model a hydraulic system a huge amount of work and many measurements performed on the real hydraulic system would be needed. Unfortunately this was not possible in this project and the hydraulic system is instead modeled from a set of standard components in Hopsan [Hop], a hydraulic simulation program, developed at LiU.

The hydraulic model, see Figure 4.4, is modeled to capture the basic behavior of a controller valve for a load-sensing system. The different components and motivations are listed below:

- The system gets its hydraulic flow from the **hydraulic pump**, (A), located at the bottom-left in the figure . The implementation of hydro-mechanical and volumetric efficiencies of the pump is not done in Hopsan, but is instead put in a separate block in Simulink.
- The system features a **pressure-relief valve**, (B), next to the hydraulic pump. If the system pressure increases above a set maximum pressure, this valve relieves some of the pressure back to the tank.

- The system is designed to operate at various pressure levels on the pump side. In order to keep the flow of oil independent of the pressure level, a **compensator valve** (C) reduces the pressure to keep the pressure drop over the orifices (D and E) at a constant level. The compensator valve uses the LS (load-sensing) pressure (E) from the heaviest load and adjusts the passed-through flow to keep the pressure at point G at a defined level above the LS-pressure, Δp .
- The **adjustable orifices** (D and E) are controlled by signals from the operator. Since the pressure drop over the orifices is constant a resulting flow can be well defined.
- In a real crane there is a load-keeping safety valve on each cylinder to prevent the load from falling, in the event of a tube breaking. In the model, this safety valve is not implemented, instead a pressure-reducing valve (G and H) is implemented, which reduces the pressure of the returning oil to a defined level. This causes the pressure drop over the orifices (D and E) to be constant for the returning as well, which enables a pressure-independent flow through the orifices.
- There are also several connections between the Hopsan model and the Simulink model. The model has outputs modeled as pressure-sensors (I and J, pump and LS-pressures respectively) and flow-sensors (K and L). The model receives flow from Simulink through ideal flow sources (M and N), it also receives signals to set the orifice-sizes (O) and pump speed (P).

4.3 Electric motor

The linear, per equivalent Y-phase, model in figure 4.5 is used to model the electric motor. The model captures the behavior of the motor well in steady state and should be sufficient for the efficiency comparison according to Umans [2014]. For the control design, the dynamics of the motor is also of interest and this is modeled by connecting an inertia to the motor. The inertia represents the rotating parts both of the motor and of the pump.

The values of the parameters of the model, see Table 4.1, have been provided by the motor manufacturer together with measurement data from different operating points. In the simulation model used in this project, see Figure 4.1, the motor voltage and the rotational speed of the rotor are input arguments and the motor current and the torque are output arguments. The model fit was investigated by inputting measured values of voltage and speed to the model and comparing the resulting current and torque with the corresponding measured values. The fit was found to be quite bad, the mean relative errors were 12.5 % for the current and 17.0 % for the torque. The parameters were therefore tuned by a least squares search algorithm where the sum of the relative least square error in current, torque and efficiency was used as goal function. The algorithm was stopped when the rate of the improvement in model fit was very low. The algorithm was

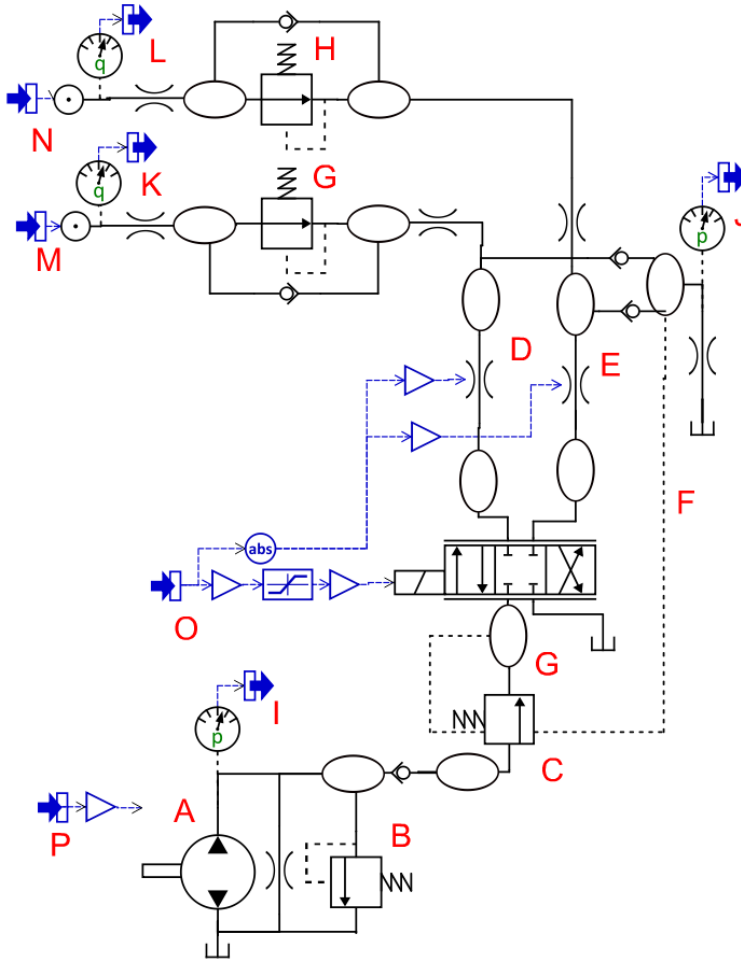


Figure 4.4: The hydraulic system modeled in Hopsan. For simplicity, only one of the four hydraulic valves is shown.

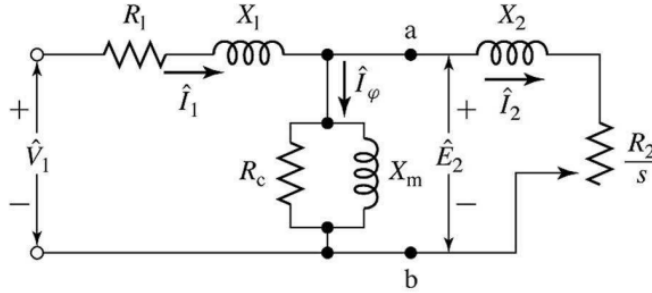


Figure 4.5: Model of the electric motor. The model is a linear, per phase equivalent model that includes winding, magnetizing and core losses.

able to decrease the sum of the relative errors by 67 % and the resulting model fit with mean values of the model errors of 5.9 % for the current and 3.9 % for the torque is considered to be sufficiently good.

Parameter	Description	Given value	Optimized value
R1	rotor resistance	2.92 mOhm	2.92 mOhm
L1	rotor inductance	54.35 μH	40.89 μH
X1 (@ 80 Hz)	rotor reactance	0.0273 Ohm	0.0206 Ohm
Rc	core losses resistance	4.45 Ohm	3.0147 Ohm
Lm	magnetizing inductance	0.98 mH	1.06 mH
Xm (@ 80 Hz)	magnetizing reactance	0.493 Ohm	0.533 Ohm
R2	stator resistance	2.02 mOhm	2.58 mOhm
L2	stator inductance	54.35 μH	38.51 μH
X2 (@ 80 Hz)	stator reactance	0.0273 Ohm	0.0194 Ohm

Table 4.1: Values of parameters of the equivalent model provided by manufacturer together with values achieved by optimization

When inputting the measurement values of speed and voltage to the model the efficiency map in Figure 4.6 is achieved. The map differs slightly from the measured map, see Figure 3.3, in the fact that the highest efficiency is centered at a higher torque level.

4.4 Inverter

The inverter, also known as a "variable frequency drive", is a controller unit that controls the speed of the electric motor by varying the frequency and amplitude of the current to the motor.

The inverter used in this project, see Section 3.1, uses a control strategy called field oriented control (FOC) to determine the output frequency and voltage. This method requires a three-phase model which is not used in the simulation model.

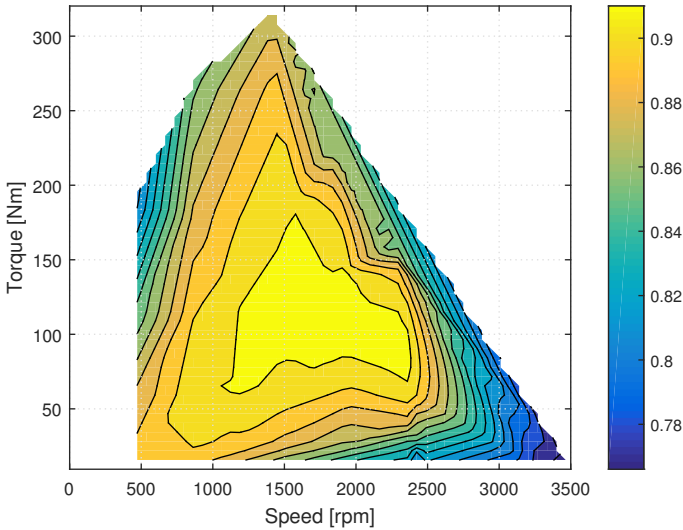


Figure 4.6: Efficiency map of the simulated motor model. The efficiency is calculated for the working points where measurements are provided by the manufacturer.

However, in steady state, the output from FOC is approximately the same value as from constant V/Hz control (explained in section 2.2) [Umans, 2014] that can be implemented in a quasi static model.

The model of the inverter is modeled to base its output voltage and frequency at a constant V/Hz ratio, with several tweaks added to handle situations of poor performance.

As can be seen in the Simulink model in Figure 4.7 the model uses the error between measured speed and requested speed (output from the controller block, see Chapter 5) to feed a PID-controller. Due to the control problem of controlling a speed (that of the motor) with another speed (the electrical frequency), the former clearly not being the derivative of the latter, the output of the PID is fed to an integrator block to complete the loop of a derivative/integrational action required for a PID-control loop to function correctly. The output of the integrator block is added to the original $rpm_{requested}$ signal, resulting in a combination of a feed forward and a feedback loop. The resulting signal is fed to the "Limit slip"-block which operate to limit the slip of the electrical motor, in order to keep the efficiency and torque within their optimal regions. A slip limiter is present in the real inverter as well.

There is also the "Current limit"-block which limits the output power if the motor current reaches above the rated current. This functionality is also present in the real inverter and plays a significant role during rapid acceleration, deceleration or high load.

The required current of the battery $I_{battery}$ is calculated using output power

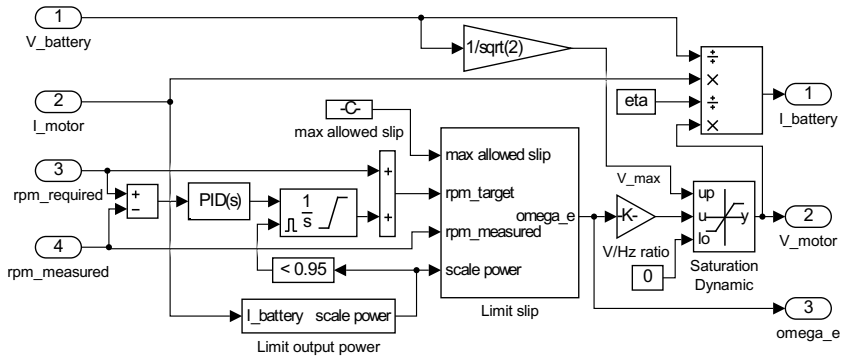


Figure 4.7: The inverter model, created in Simulink. The model uses the rpm signal from the controller together with the measured rpm signal to control the output voltage and frequency of the current to the motor.

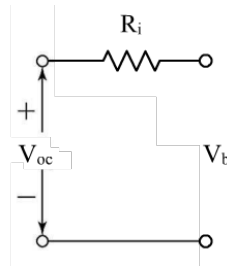


Figure 4.8: Equivalent circuit of the battery, modeled as an internal open-circuit voltage as well as an internal resistance, resulting in a linear, current dependent voltage drop.

and a pre-defined internal efficiency η . The efficiency is assumed to be constant, a simplification of the real inverter where the efficiency is actually dependent on the load. The load dependency is only significant when the inverter is operated far below its rated power so the simplification will probably not affect the performance of the system at normal operation.

The output voltage V_{motor} is (due to obvious reasons) limited to the maximum available voltage from the battery. Since V_{motor} is an RMS-value, the value is limited to a maximum of $V_{battery}/\sqrt{2}$.

4.5 Battery

The battery is modeled as an equivalent circuit (see Figure 4.8) with a potential and an internal resistance. The internal resistance is important for the comparison to include in the model since a less efficient system will require a higher current from the battery in order to provide the same power as a more efficient

system. A higher current will result in a higher loss in the battery due to the internal resistance and this will affect the overall efficiency of the system. In reality, the potential of the battery is a function of the state of charge but during the short drive cycle that will be used to compare the systems in the project the variation will probably not be significant. Even if it was, it would affect the systems equally.

To determine the internal resistance of the battery a test was performed on the test rig. A load was varied so that the current drawn from the battery varied between 0 and 520 A. The battery voltage was then measured for several operating points. A plot of the voltage drop due to the internal resistance as a function of current can be seen in Figure 4.9. Since the relation appears to be almost linear, the internal resistance is calculated as the least square solution to $IR_i = U_{Ri}$.

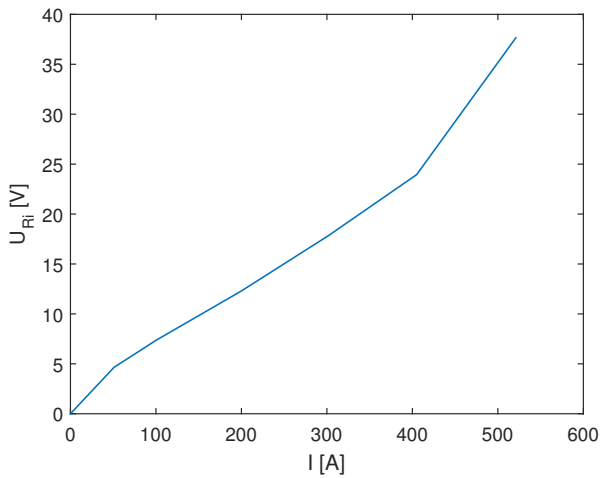


Figure 4.9: Measured voltage drop in the battery as a function of current. The voltage drop is approximately a linear function of the current.

5

Control

In this chapter different control strategies used for controlling the hydraulic flow and pressure are addressed.

If a conventional hydraulic pump (with a mechanical controller) is to be replaced by an electrically controlled fixed pump, there are several possible control strategies available, each dependent in different magnitudes on how many of the system properties that need to be measured.

The conventional strategy and the strategies proposed in this project are presented in Table 5.1 together with the input signals required for each strategy. The four strategies that can be implemented with a fixed displacement pump are investigated with the model of this project and are described in the following sections. An evaluation of the different strategies is made in Section 6.2.

5.1 Pressure feedback control

The simplest feedback controller is a PID-controller that uses the difference in pressures as the error input. This requires only two measuring points (actual and load-sensing pressures) which is a cheap implementation, but it might suffer

Name	Required input signals
Conventional, var. displ. pump	p_{pump}, p_{LS} (mechanically sensed)
Pressure feedback control	p_{pump}, p_{LS}
Flow feed forward control (FF)	Operator commands (OC)
FF + complementary pressure feedback	OC + p_{pump}, p_{LS}
True flow control	OC + individual load pressures

Table 5.1: Comparison between the proposed control strategies

from poor performance or instability issues.

The controller is implemented in Simulink, see Figure 5.1, with a standard PID-controller block which outputs a signal corresponding to a hydraulic flow. The flow is converted to a corresponding rotational speed of the pump, using the pump displacement. This allows for easy testing of different pump sizes, without the need to change the PID parameters.

As seen in the figure, a maximum limit of pressure is present to prevent the controller for exposure of any pressures higher than the rated maximum system pressure. This is used to prevent the controller from outputting a flow that would only pass to the hydraulic pressure reducing valve, during maximum load.

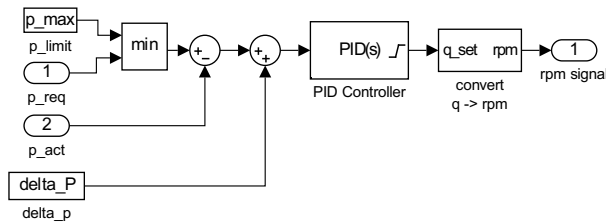


Figure 5.1: The pressure feedback controller in Simulink. The controller uses the required pressure together with the actual pressure to control and output the rpm signal to the inverter.

The rpm-signal from the controller is sent to the inverter which controls the speed of the pump to the desired speed.

5.2 Flow feed forward control

The operator of the crane controls the crane by levers, shifting the position of one or several of the valves to the different functions, diverting the oil flow to these functions.

By measuring the lever positions of the operator a resulting flow demand can be calculated, using the pre-defined flow characteristics of the valves. This flow can be directly fed forward to control the speed of the hydraulic pump.

The biggest advantage of using a feed forward controller is that it can be made arbitrarily fast without risking the instability issues that are introduced when speeding up a feedback controller. The feed forward controller can be set to simply forward the actual flow demand as a required speed. The only delay in the power pack will then be due to the maximum power of the inverter together with the inertia of the electric motor and the hydraulic pump.

A disadvantage of simply feeding forward the valve positions is the risk of outputting a too high flow, due to model errors. When outputting a too high flow the hydraulic compensator valves will close (to keep the flow constant), and as a result, the pressure on the pump side will increase rapidly. A high pressure

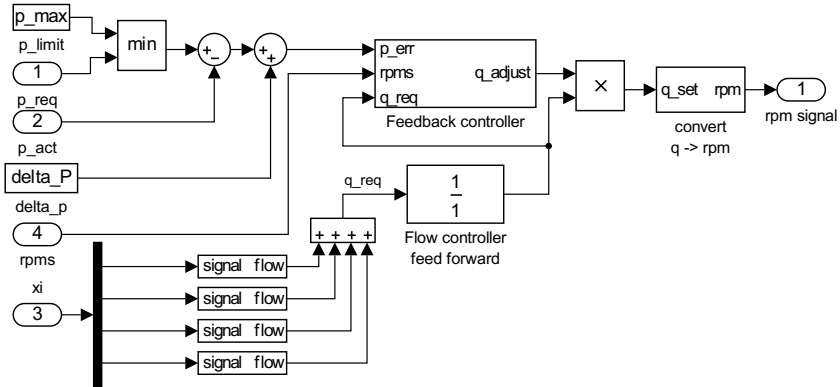


Figure 5.2: The feed forward controller together with the complementary feedback controller in Simulink. The feed forward block uses a required flow, calculated from the operator commands x_i . The output of the feed forward block is modified by the pressure feedback block, which uses the required and actual pressures as inputs.

on the pump side causes large unnecessary losses, both in the hydraulic pump (that has to deal with a large pressure difference, causing bad efficiency) and the compensator valves (which lower the pressures by converting the excess pressure to heat). If on the other hand, the feed forward controller outputs a too low flow, due to model errors, the hydraulic pressure at the pump will decrease until the compensator valves opens up completely (to try to keep the flow constant) and equilibrium ensues. This will result in a lower hydraulic flow than expected, but is not dangerous or ineffective, the movement of the crane will only be slower than expected.

5.2.1 Complementary pressure feedback

The risk of the feed forward control outputting an incorrect flow due to model errors, described in the previous section, can be avoided by implementing a complementary feedback controller that uses the measured pressures to modify the feed forward signal. The complementary feedback controller can be made much slower than the standalone feedback controller discussed in Section 5.1 since it doesn't have to be able to have a fast step response, the feed forward controller takes care of that. This implies that the controller can be made more robust which makes it better suited for controlling highly nonlinear systems, such as this hydraulic system.

The implementation of the feed forward controller together with the complementary pressure feedback controller can be found in Figure 5.2. It is worth noting that the output of the feedback controller is multiplied with the output of the feed forward controller, instead of the two signals being added together. The advantage of this becomes apparent when the operator quickly sets the valve po-

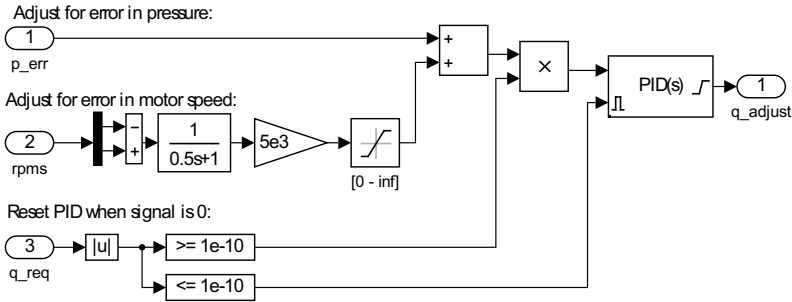


Figure 5.3: The internal workings of the complementary feedback controller. The PID-controller primarily uses the error in pressure to output the flow adjustment value, but is also using the error in motor speed (due to the inverter being unable to control the motor) to prevent integrator wind-up.

sitions (i.e. the required flow) to zero. If the values would be added together the FF-signal would return to zero arbitrarily fast, but the FB-signal wouldn't return to zero until after a while (due to the pressure spiking). When the signals are multiplied instead the resulting signal will return to zero arbitrarily fast, which is desirable. The fact that the contributions from the two controllers are multiplied rather than added requires some modifications of the reasoning regarding the correlation between the model error and the feedback signal in Section 2.1.4. $q_{ff} + q_{fb}$ in Equation 2.4 has to be replaced by $q_{ff} \cdot q_{adjust}$, where q_{adjust} is the dimensionless output of the feedback controller. This gives the relation in Equation 5.1 and further, the expression for q_{fb} in Equation 5.2. Since the conclusion from Section 2.1.4 is that q_{fb} can be used as a measure of the model error in the additive case it now holds that $q_{ff}(q_{adjust} - 1)$ can be used as the same in the multiplicative case. q_{ff} depends only on the required flow (i.e. *not* on the model error) and is thus constant at a working point. It follows that q_{adjust} alone can be used as a measure of the model error and that the structure of the adaptive parameter set proposed in Section 2.1.4 is still valid.

$$q_{ff} + q_{fb} = q_{ff} \cdot q_{adjust} \quad (5.1)$$

\Leftrightarrow

$$q_{fb} = q_{ff}(q_{adjust} - 1) \quad (5.2)$$

The feedback controller, seen in Figure 5.3, consists of a PID controller that uses a sum of two signals. The first signal is the measured error in pressure as previously discussed.

The second signal is an input that is used to cope with situations that arise when the inverter (or the electric motor) is unable to control the speed of the electric motor, often caused by limitations in available power or voltage from the battery. When the inverter/motor/pump is unable to provide the speed (or rather the hydraulic flow) required, the system pressure drops, which causes p_{err} to rise. This causes the feedback controller to raise inappropriately and later, due to integrator wind-up, temporary but still unpleasant oscillatory behaviors when the system returns to normal operation. To prevent the integrator wind-up the input error signal is adjusted with the error between the actual and the required speed of the motor. When the measured speed of the motor differ too much from the required speed the PID controller will adjust down the required motor speed, so that the whole system is more balanced later when the situation changes or more power is available.

The reset feature in the lower part of Figure 5.3 should also be noted. This resets the value of the PID controller to 1 when the controller is idle and makes separate movements independent of previous movements, which is desirable when different movements have different characteristics.

5.2.2 Adaptive parameter set

When utilizing a feed forward type controller the performance is limited by the understanding of the model. Any errors in the model will directly result in an error in the feed forward control signal. As described in Section 5.2, a control signal that is too high will quickly result in a pressure build-up in the system, with large energy losses as a result.

By utilizing an adaptive parameter set to calculate the required flow (see the theory in Section 2.1.4) the feed forward controller will be tuned to forward the average flow required in most situations, ideally rendering the complementary feedback unnecessary.

The adaptive parameter set is implemented in Simulink as a separate component, see Figure 5.4. The block takes the operator signals as well as the flow-adjusting signal from the feedback controller as inputs and outputs a set of parameters used for calculating the required flows.

Inside the adaptive parameter set block, displayed in Figure 5.5, the four functions are separated and takes as inputs the operator signal, x_i , and the flow-adjusting signal, q_{adjust} , as well as a reference set of points of signal magnitudes of which to calculate parameter points at. For each function, a parameter k corresponding to the current signal magnitude is returned.

The "signal magnitudes" is a vector consisting of different possible values of the operator signal, for example $[-1 -0.75 -0.5 -0.25 0 0.25 0.5 0.75 1]$. At each of the points specified by this vector, a parameter state is created, corresponding to an adjustment of the model at this specified signal value. When an operator signal is currently between some points, the returned parameter value will be calculated by a mix of the nearby points.

In the function-specific adaptive parameter set block, see Figure 5.6, where the actual work is done, the operator signal is subtracted from the magnitude

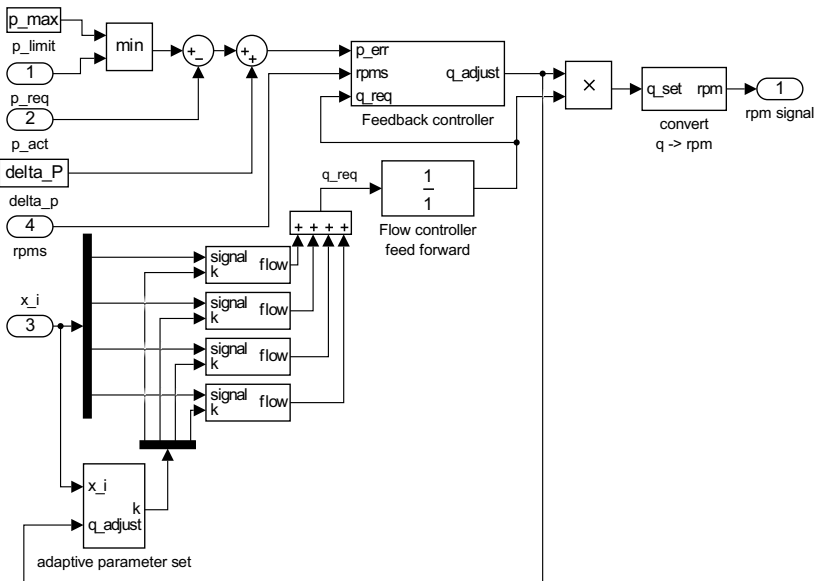


Figure 5.4: The flow feed forward and pressure feedback controllers, with adaptive parameter set block added at the bottom. The adaptive parameter set uses the output from the feedback controller together with the operator signals x_i to adjust and output its parameters, used to calculate the required flow.

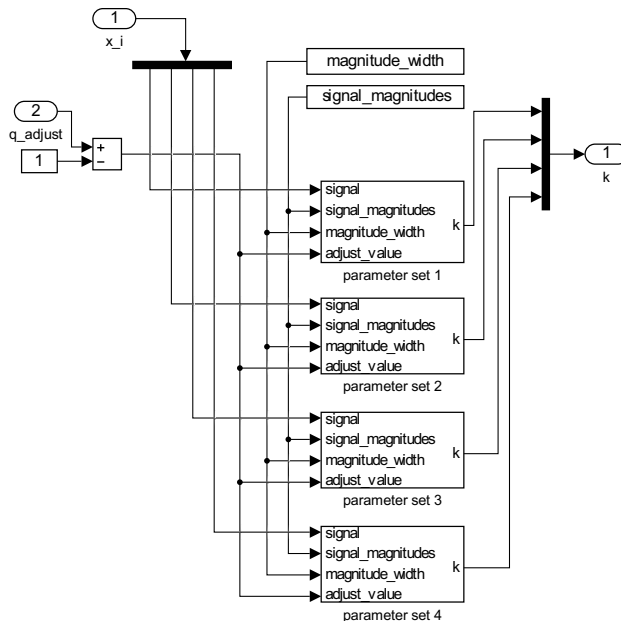


Figure 5.5: The internal workings of the adaptive parameter set block. The operator signals and the flow adjustment values are distributed to four sub-systems, each associated with one of the four different crane functions. The subsystems are further explained in Figure 5.6.

vector, resulting in a vector containing weights depending on the distances from the signal value to the parameter magnitude. The vector is then used as a base for influencing the weighting of the different parameter points. An example of the weight distribution is displayed in Figure 5.7, for a parameter with magnitude of 50 %.

The flow adjusting value combined with the magnitude weight is used to adjust the parameter state. For example, a negative value of the adjusting value will cause the parameter state to fall, but thanks to the combination with the magnitude weights, only the states corresponding to signal values currently used will be affected. This is desirable because it is probably the signal magnitudes currently in use that are responsible for any adjustments needed to be made, and thus it is these points that should be adjusted.

The magnitude weights are also used to create a signal magnitude dependent, weighted average of the parameter set. This average is then output and will be used for adjusting the calculated required flow used by the feed forward controller.

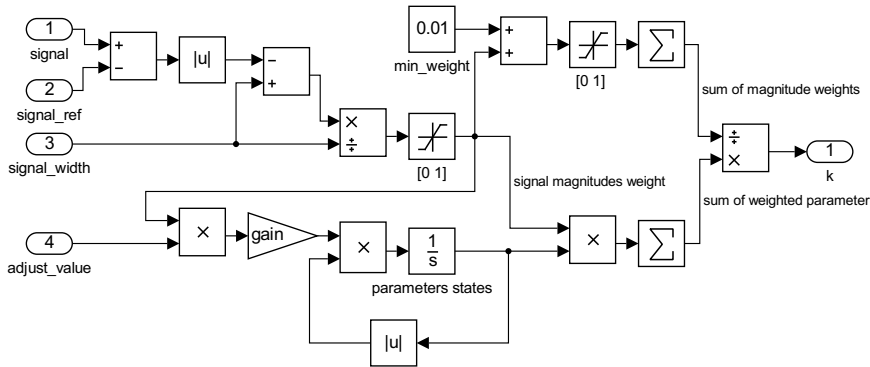


Figure 5.6: The internal workings of a parameter set block. The operator signal is used together with the adjustment value to adjust some of the values in the parameter set. A weighted average of the parameter set is then output.

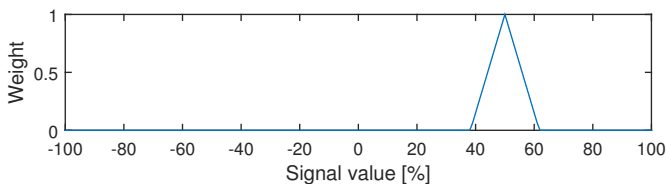


Figure 5.7: Example weight distribution for the parameter at 50 % in the parameter set. Note that there is an equivalent weight distribution for each parameter in the parameter set.

The *gain* constant is used to scale the flow adjusting value to set how fast the

parameter states should be adjusted. The constant is set to a low value, so that parameter states are only slightly adjusted during a single duty cycle. This way the parameter states will approach an average value (this happens after many duty cycles) that will minimize the usage of the feed controller. A higher value of *gain* will make the parameter state adjustment faster, but will also increase the risk of local optimization and within-cycle impact, which is undesirable.

5.3 True flow control

One of the goals in this project is to examine different ways of increasing the efficiency of the overall system. One way of increasing the efficiency in the hydraulic system would be to decrease the system pressure and avoid unnecessary pressure losses. As described in the theory (Section 2.1.4) the system pressure can be decreased by forcing the valve of the heaviest load to open fully, rendering the compensator valve and the constant-flow function paralyzed. The flow of the function with the heaviest load is instead controlled by the hydraulic pump and the feed forward controller.

To achieve a correct behavior, some conditions have to be fulfilled:

- Since the Δp of the hydraulic system won't be at a fixed level anymore, the complementary feedback controller (which uses this for control) must be disabled.
- The feed forward controller requires a well calculated required flow. Erroneous flow will result in a too slow movement (when too low) or a drastic increase in system pressure (when too high).
- The pressures of the individual loads have to be measured, in order to determine which of the loads that is the heaviest one.

The true flow control is implemented in Simulink as a block that intercepts the valve signals, x_i , modifies the appropriate signals and outputs the new signals, $x_{i\text{adjusted}}$, that are to be sent to the valves. The resulting controller, including the flow feed forward controller, the adaptive parameter set and the additional valve signal adjustment block, is displayed in Figure 5.8.

Inside the valve signal adjustment block (see Figure 5.9) the individual pressures p_i are compared in order to determine which function is the heaviest one. The result of this evaluation, together with the operator signal x_i and the active dampening signal $x_{\text{dampening}}$ is fed to subsystems which outputs the adjusted signals.

The subsystem (see Figure 5.10) is designed to only activate the "True flow control" concept when certain requirements are fulfilled, to avoid overall bad controller performance or stability issues during change of modes. During initial simulations, bad performance was discovered during zero-crossings of the signal. This was derived to be caused by the discrete change of valve position (-100 % to 100 %). The controller performance was also worsened during mode changes, i.e. changes in whether the function is working in "true flow control mode" or not.

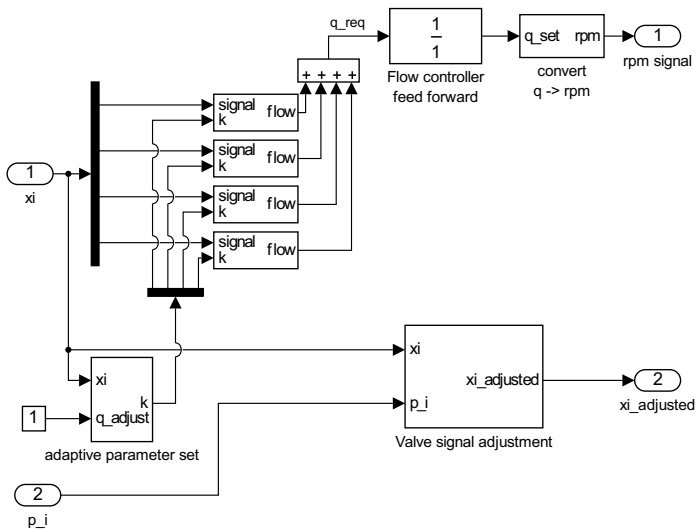


Figure 5.8: The previously mentioned feed forward controller and the adaptive parameter set, with the valve signal adjustment block added. The valve signal adjustment block uses the operator signals and a vector of load pressures to output the (possibly) adjusted valve signals.

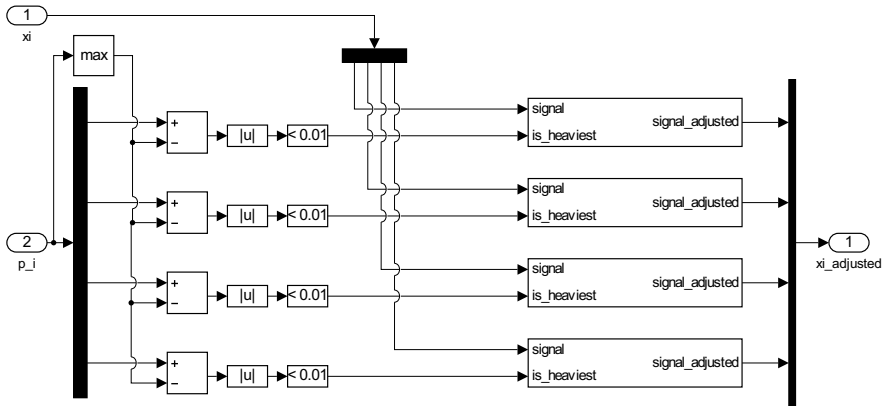


Figure 5.9: The internal workings of the valve signal adjustment block. The load pressures are compared to determine which is the heaviest. The four subsystems are further described in Figure 5.10.

To cope with these issues a strategy is made up to only allow for the "true flow control" to be activated if the following statements have been true for a certain period of time:

- No zero crossings in the signal have occurred
- The function is the heaviest one

Also a first-order transfer function is added to soften the transition modes. The output of the transfer function (the "degree-of-activation") is a value between zero and one which is used to produce a weighted mix between the original (unmodified) signal and the modified (forced to -1 or 1 depending of sign) signal.

During a drive cycle, the degree-of-activation will gradually increase (up to fully activated) for one of the functions until one of the requirements previously listed no longer is true, then it will return to zero.

As is seen in Figure 5.11, during periods of sustained movement in a single direction (0-35 s and 55-75 s) the true flow control is activated a large part of the time. During periods of non-sustained or directional changes, the true flow control isn't activated as much.

5.4 Operator simulation

When evaluating the performance of the controllers together with the crane there is a need for running the crane in a pre-defined and repeatable cycle in order to

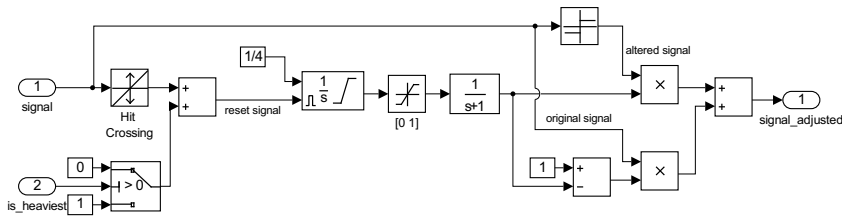


Figure 5.10: The valve signal adjustment block subsystem which outputs either the original or an adjusted signal, depending on certain requirements. The requirement calculation uses the original signal as well as a Boolean value indicating whether the associated load is the heaviest or not.

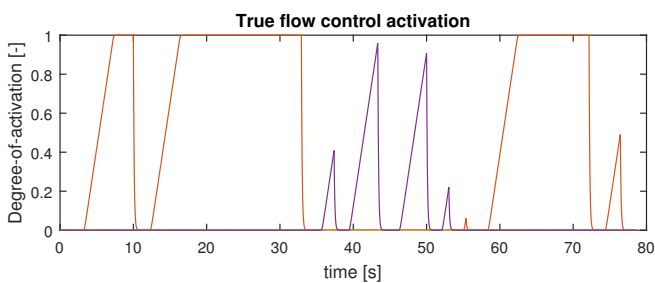


Figure 5.11: The degree-of-activation of the true flow controller during a drive cycle. Between 35-55 s the true flow control is partly activated for the second boom function, otherwise it is partly or fully activated for the first boom.

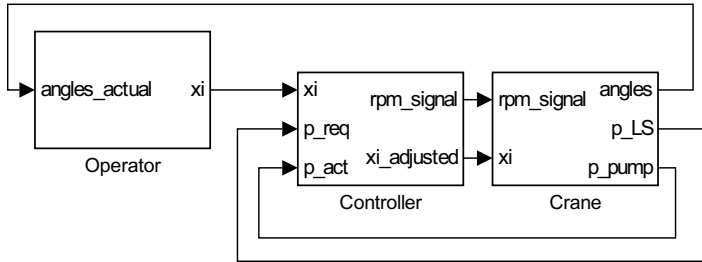


Figure 5.12: The operator block and its relations to the controller and crane blocks. The operator block uses the measured angles of the crane as well as an internal pre-set drive cycle and outputs its operator signals to the controller block.

be able to compare different runs with each other. The crane is operated with four signals indicating a desired speed for each of the functions. A first approach to this would be to define a cycle consisting of steps and ramps in the control signals. However, if the step response of the crane (i.e. the hydraulic power pack) is changed between runs, the resulting angles of the crane would not be consistent between runs - rendering the drive cycles incomparable.

To create a scenario with repeatable results, an "operator" controller is implemented as a separate block in Simulink. The operator block and its relations to the other parts of the system model can be viewed in Figure 5.12. The operator controller is meant to simulate the actions of a real operator, using the actual angles of the crane, comparing them with the target angles provided by a pre-defined drive cycle and outputting control signals to the controller block.

To ensure a repeatable drive cycle it is desirable that the crane follows a certain path and does not divert from the path too much, since this would allow for the crane to "take a shortcut" to the target position, resulting in a lower power consumption unrelated to the hydraulic system performance.

If using a fixed drive cycle with target positions associated with fixed time points, it would be impossible to make certain that the crane actually follows the path, since there might be limitations in available power or other controller-related issues making it impossible to follow the path fast enough. To cope with this the cycle time is not fixed, instead the cycle uses a "time variable" that increases at different rates, depending on how well the crane is currently following the position target. If the crane has trouble following the path there will be a big error between the current and actual position. A big error will slow down the rate of which the "time variable" is increased, causing the drive cycle to slow down and allow the crane to "catch up", without allowing it to take any shortcuts in the pre-defined path.

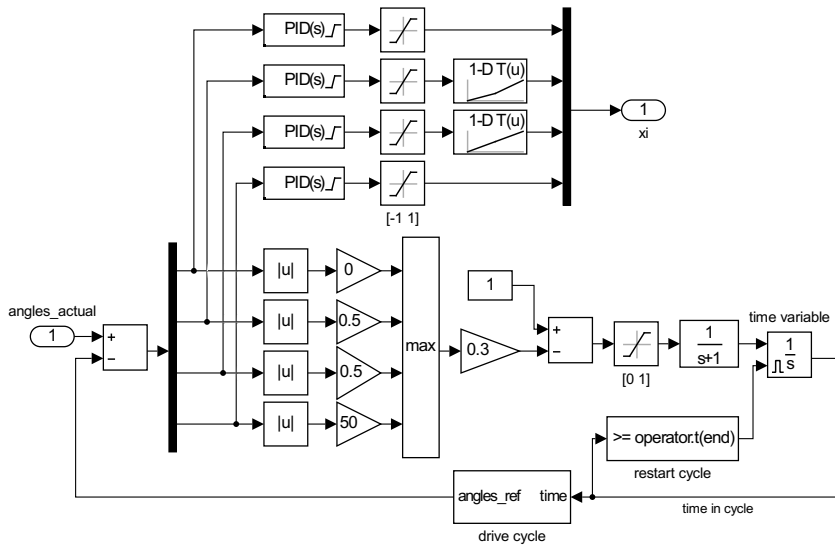


Figure 5.13: The internal workings of the operator block. The reference angles from the drive cycle block (at the bottom) is compared to the measured angles and fed to PID-controllers, generating output operator signals (at the top). The errors in angle are also used to determine the speed of the drive cycle, slowing it down if the errors in angle are too high.

The operator block (see Figure 5.13) takes the current angles as input signals and creates an error together with the target angles obtained from the drive cycle. The errors are directed to the PID-controllers which control the crane movement. The error of largest magnitude is also used to slow down the input of the "time variable" integrator, effectively causing the drive cycle to slow down in case of large errors.

The operator controller proved to be able to successfully control the motions of functions two, three and four (boom 1, boom 2 and the extender). Function one (rotation of the crane) however proved to be very difficult to control due to a severe signal delay from control signal to measured movement. Since the operator was able to control the other three functions well it was decided to use a drive cycle featuring only movements of the three working functions. The results from simulations are expected not to be affected by running the crane on three functions only and should be applicable to the crane as whole.

5.5 How to investigate the robustness of the controllers

To be able to mathematically investigate the robustness of the controllers mentioned above a mathematical model of the controlled system must be produced. Many parts of the model have nonlinear behaviors and it is improbable that the model can be approximated by a linear model that can be used to investigate the robustness for the whole working area of the application. The purpose with the investigation in this section is to find out whether the system can be linearized around certain operating points. If the system can be approximated by a linear model in a certain area, the robustness of the controllers in this area can be investigated mathematically.

A schematic of the system with pressure feedback can be found in Figure 5.14. The transfer function from the reference value (required pressure at the pump side, $p_{req} + \Delta p$) to the controlled signal (motor speed, n) when using the pressure feedback controller F_{fb} can be derived by Equations 5.3 to 5.5. G is the unknown transfer function of the inverter, the electric motor, the hydraulic system and the mechanical model combined, i.e. from n to p_{act} . G will have to be estimated. When using feed forward control with complementary pressure feedback the expression for n in Equation 5.3 will be different but G will still have to be estimated.

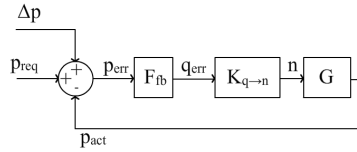


Figure 5.14: Schematic of the feedback system. The reference signal is the required pressure at the pump side and feedback signal is the actual pressure.

$$n = K_{q \rightarrow n} F_{fb} p_{err} = K_{q \rightarrow n} F_{fb} (p_{req} + \Delta p - p_{act}) \quad (5.3)$$

$$p_{act} = Gn \quad (5.4)$$

$$5.3, 5.4 \Rightarrow$$

$$n = \frac{K_{q \rightarrow n} F_{fb}}{1 + K_{q \rightarrow n} F_{fb} G} (p_{req} + \Delta p) \quad (5.5)$$

The pressure outputs of the mechanical model depend on the positions of the different parts of the crane. Since the positions change when a flow is applied to

the system the system doesn't stay around a single working point. To get around this and to be able to find a transfer function for a working point, the pressure outputs are measured for a certain position and then set to those constant values. The mechanical model is thereby omitted from G .

The rotational speed n is not the only input to the system, the operator signals x_1 , x_2 , x_3 and x_4 also affect p_{act} . To obtain a SISO system from n to p_{act} , an operating point for the operator signals is chosen where valves 1 and 4 are closed and valves 2 and 3 are fully open. To estimate the transfer function G , simulations of the systems are made for different input values of n and the response in p_{act} is measured.

When a step is made in n from 700 to 800 rpm at 4 s a response in p_{act} is obtained according to the solid line shown in Figure 5.15. A nonlinear behavior can be observed since the system responds faster to a decrease in speed than an increase. Furthermore, when trying to approximate the system G by a second order transfer function, the dashed line in the figure is obtained as pressure response when the speed is changed from 700 to 800 rpm. The gain of the transfer function is fitted to the pressure level corresponding to 700 rpm and as can be seen in the figure the gain does not fit the pressure level corresponding to 800 rpm. This indicates that the gain depends of the magnitude of the speed value. The error when using the linear transfer function model is not very big however and the approximation of a constant gain could be reasonable.

However, the previously discussed linearization prove to be very erroneous if the speed is significantly higher or lower than the range 700-800 rpm. Figure 5.16 displays the step response in pressure from the model, together with the estimated pressure response from the same transfer function used in Figure 5.15 when a step in speed from 600 to 700 rpm is made. The same nonlinear behavior can be observed when the pressure level of a second order transfer function is tuned to match the pressure level corresponding to a speed of 800 rpm and a step in speed is made from 800 to 900 rpm, see Figure 5.17.

The conclusion from this investigation is that the system is highly nonlinear and that in order to approximate it by linear models around several working points the speed windows in which each model is valid will have to be very small. Since the motor is supposed to work in a speed range of 3000 rpm it is not reasonable to define a linear model for each range of about 20 rpm. The lack of suitable transfer function models of the system makes a mathematical analysis of the robustness of the controllers difficult. The amount of noise or model errors that the controllers can handle will therefore be investigated by simulations.

5.6 Evaluation of controller performance

How well a controller performs is defined by several *performance factors* and by how well they handle *disturbances*. Different sets of controller parameters (P, I and D values of the PID-controllers in the pressure feedback and the complementary feedback) are tested on the reference drive cycle (see Section 6.2). The resulting values of the *performance factors* are measured and logged between the

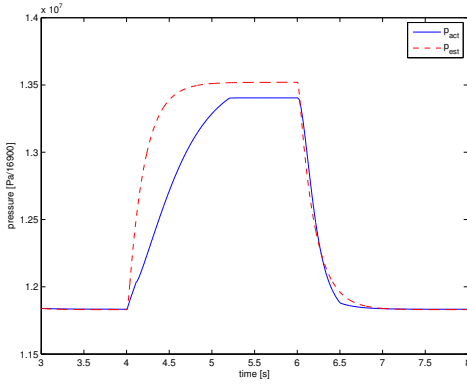


Figure 5.15: Pressure response from transfer function fitted to a pressure level corresponding to 700 rpm (dashed) compared to pressure response from model for a step in speed from 700 to 800 rpm.

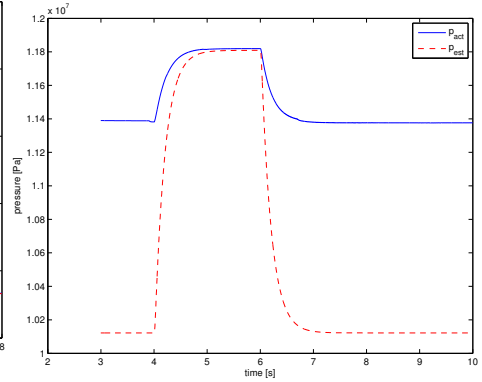


Figure 5.16: Pressure response from the same transfer function as in Figure 5.15 (dashed) compared to pressure response from model for a step in speed from 600 to 700 rpm

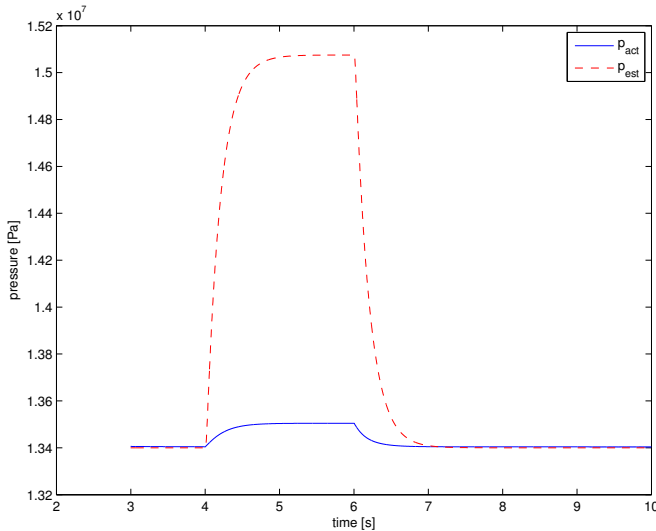


Figure 5.17: Pressure response from transfer function fitted to a pressure level corresponding to 800 rpm (dashed) compared to pressure response from model for a step in speed from 800 to 900 rpm

sets. The parameter sets are then tested with different *disturbances* during the drive cycle. The different controller strategies (pressure feedback, flow feed forward with complementary feedback and true flow control) and different version of those can then be compared according to reference following, noise sensitivity and oscillative behavior. See Appendix A for a more detailed description of the process of selecting the best controllers and how the *performance factors* and the *disturbances* are defined.

6

Results

This chapter is divided in two main sections, *Measurements on test rig* and *Controller strategy performance*. In the first section the results obtained from the test rig are presented. These results focus on energy efficiency. In the second section the results from the simulations of the Simulink model are presented. These results, as the title suggests, focus on controller performance.

6.1 Measurements on test rig

In this section the results from the *drive cycle tests* defined in Section 3.2 are presented. The drive cycle is also defined in Section 3.2.

6.1.1 Performance during drive cycle - configuration 1

The noisy signals in Figure 6.1 are the unfiltered values of the measured pressure and flow during the drive cycle from the test with a pump speed of 2000 rpm. The unfiltered signals from the test with a pump speed of 2500rpm follow the same pattern.

To be able to calculate the efficiency and compare it with the second configuration the signals had to be filtered, the filtering method is described in Section 6.1.2. The filtering prevents any analysis of the transient performance of the system, but for an efficiency comparison only the steady state-like level is important. The filtered signals are displayed together with the unfiltered signals in Figure 6.1. In the zoomed in parts of the figure it can be seen that the filtered version of the signals follow the steady state levels of the original signals, if the noise pulses are disregarded.

In Figure 6.2 the filtered signals of the two tests are displayed together with the drive cycle values. The reference following is deemed to be sufficiently good.

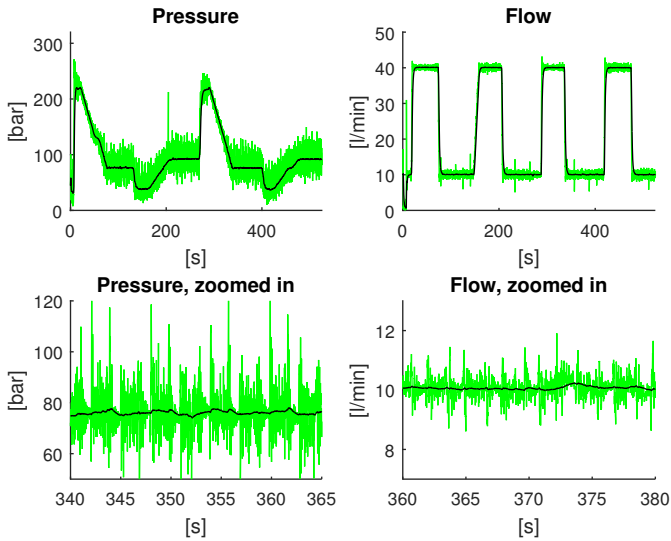


Figure 6.1: Original and filtered measurements of pressure (left) and flow (right) during the test drive cycle.

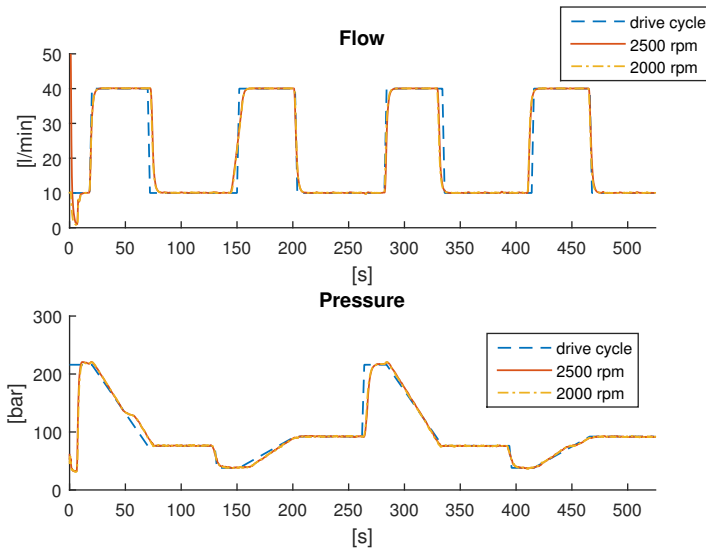


Figure 6.2: Filtered measurement signals of flow (upper) and pressure (lower) compared to the reference drive cycle values. As can be seen, the flow and pressure follow the references very well.

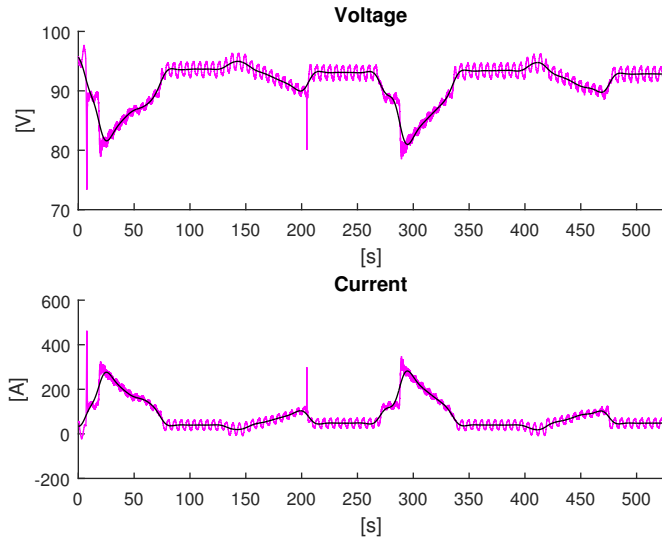


Figure 6.3: Original and filtered measurements of battery voltage (upper) and current (lower). The filtering manages to remove the high frequent measurement noise.

The battery voltage and current were also measured to be able to calculate the efficiency of the system. The noise of those signals is a constant high frequency noise that can be filtered by a normal low pass filter. Original and filtered versions of those signals from the test with a speed of 2000 rpm are displayed in Figure 6.3. As described in Section 4.5 the voltage drops almost linearly with increasing current.

The efficiency of the test rig system (excluding the battery) can be calculated from the filtered measured data according to Equation 6.1, where p_{pump} and q_{pump} are the measured pressure and flow and V_b and I_b are the measured voltage and current from the battery.

$$\eta = \frac{P_{out}}{P_{in}} = \frac{p_{pump}q_{pump}}{V_b I_b} \quad (6.1)$$

The efficiencies of the two tests are displayed in Figure 6.4 together with the output power. Note that the efficiency is significantly higher for high loads than for light loads, $\sim 60\%$ and $\sim 35\%$ respectively. Note also that the efficiency for the test with a speed of 2000 rpm is higher than that for the test with a speed of 2500 rpm for light loads.

6.1.2 Performance during drive cycle - configuration 2

The measurement noise during the tests with configuration 2 was even higher than during the tests with configuration 1. Unfiltered measurements of pressure

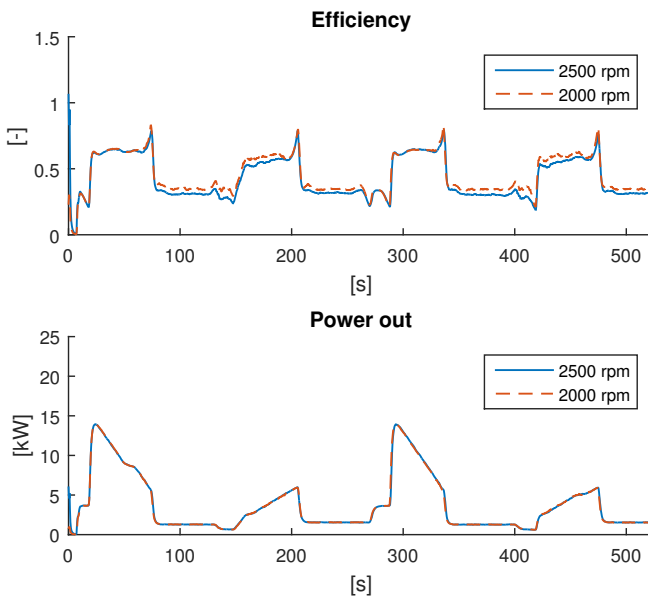


Figure 6.4: Calculated efficiency (upper) and output power (lower) during the two tests. The efficiency is significantly lower during periods of low power output.

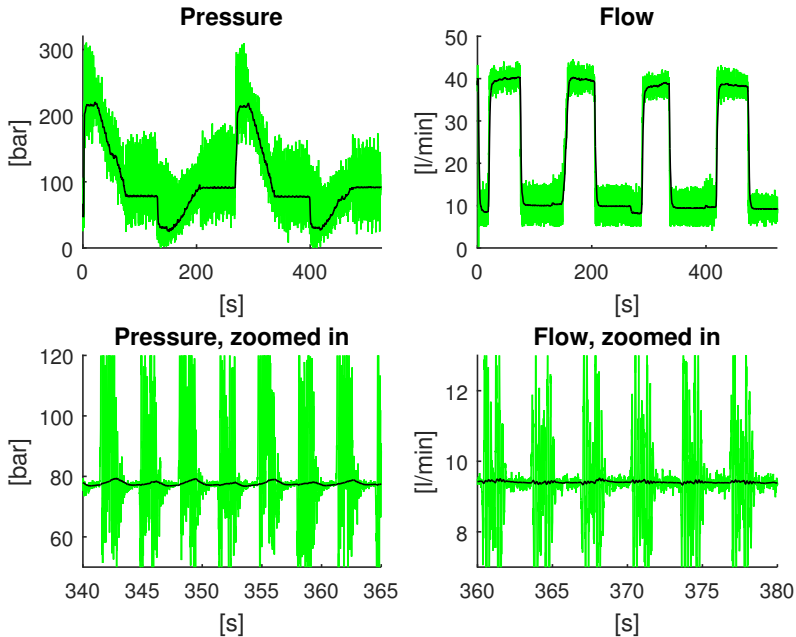


Figure 6.5: Original and filtered measurements of pressure (left) and flow (right). Note that the magnitude of the noise is periodic and that the average values of the noisy signal parts are offset to the values of the non-noisy parts.

and flow of one the two tests are shown in Figure 6.5. As can be seen in the zoomed in parts of the figure, the noise consists mostly of periodic pulses. This periodic noise can be removed by a filtering method that calculates a weighted gliding average for each sample in the signal. The weight for each sample is the inverse of the amount of noise in that point. The amount of noise is defined as the gliding-average deviation from a low-pass filtered signal. The noise-reduced signals are displayed together with the original signals in Figure 6.5. When zoomed in, it is noticeable that the steady state levels of the filtered signals follow the original signals if the periodic noise is disregarded.

In Figure 6.6, the filtered signals from the two measurements are plotted together with the drive cycle. The reference following is deemed to be sufficiently good.

The measurements of voltage and current drawn from the battery have the same appearance as during the measurements with configuration 1 and can thus be well smoothed by the low pass filtering and used for the efficiency calculation.

The efficiencies, calculated with filtered measurement signals according to Equation 6.1, are displayed in Figure 6.7. The output power is also displayed so that the efficiency can be related to the level of output power. Note that the difference in efficiency between the sections with high and low loads, $\sim 70\%$

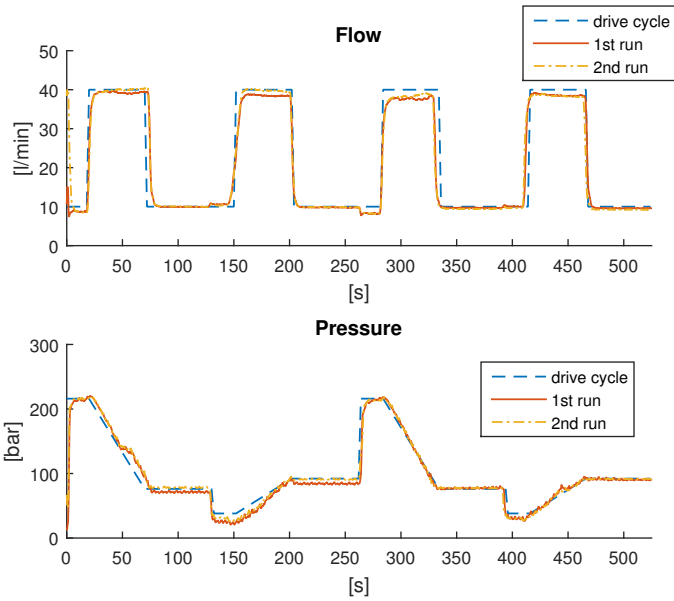


Figure 6.6: Filtered measurement signals of flow and pressure compared to the reference drive cycle values. As can be seen, the flow and pressure is following the references quite well.

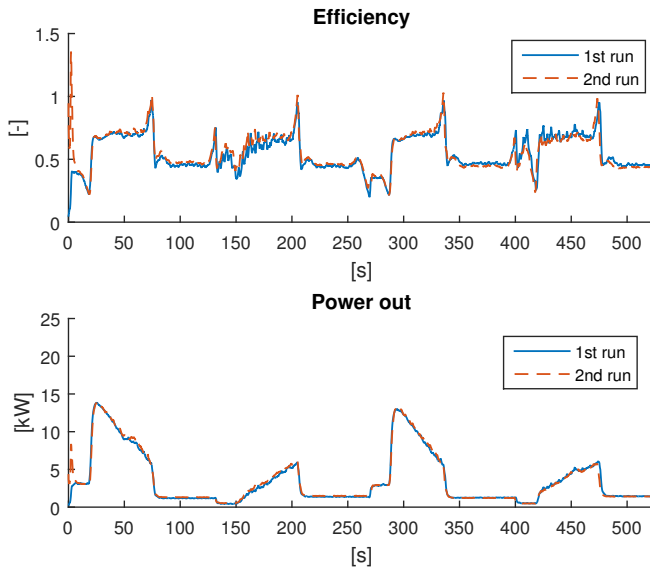


Figure 6.7: Efficiency and output power of the two test runs. The efficiency is notably lower during periods of low power output, but still higher than in Figure 6.4.

and $\sim 47\%$ respectively, is somewhat lower than the difference for the tests with configuration 1.

6.2 Controller strategy performance

The purpose of the simulation model is to evaluate the performance of different controller strategies on the system with configuration 2. In the following sections the performance of the three strategies *pressure feedback*, *flow feed forward with complementary pressure feedback* and *true flow control* will be presented and compared according to different criteria. One controller from each strategy will be investigated. The selection of these controllers is made according to the method described in Appendix A and represents a tradeoff between the criteria discussed below.

An important part of the comparison is to compare the behavior of the different controllers during a pre-defined reference drive cycle. The reference drive cycle used in this project consists of two consecutive lifts of the load, first with the crane largely extended horizontally and then with the crane more folded, see Figure 6.8. The drive cycle is realized by the operator controller block, see Section 5.4 to make sure that different runs are comparable with each other.

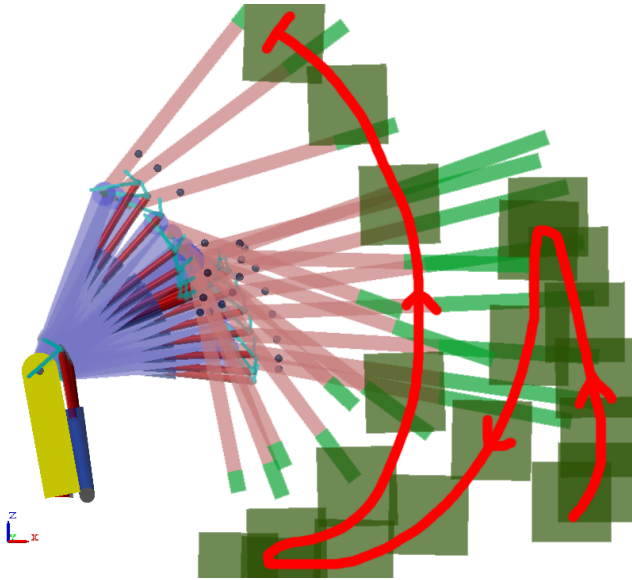


Figure 6.8: Visualization of the positions of the crane during the reference drive cycle used in simulations.

6.2.1 Energy efficiency

Since the controllers aren't able to follow the drive cycle exactly, the output energy from the systems differs a little between the simulations with the different controllers (from 0.0495 kWh to 0.0510 kWh). This implies that it is better to compare the energy efficiency than the energy consumption. The efficiencies of the power pack, the hydraulic system and the two combined are presented in Table 6.1. It can be noted the efficiency of the power pack is very similar for all controllers but that the efficiency of the hydraulic system is significantly higher for the true flow controller than the other two. As a consequence, the total efficiency for the true flow controller is also higher than for the other two.

Strategy	Efficiency power pack [%]	Efficiency hydraulic system [%]	Efficiency power pack + hydraulic system [%]
Pressure feedback	63.3	36.0	22.8
Flow feed forward	63.1	35.5	22.4
True flow control	63.3	40.5	25.6

Table 6.1: Efficiencies of subsystems during a drive cycle. The charge/discharge efficiency of the battery is included in the efficiency of the power pack. Note the increased efficiency of the hydraulic system during "True flow control", thanks to lower pressure losses.

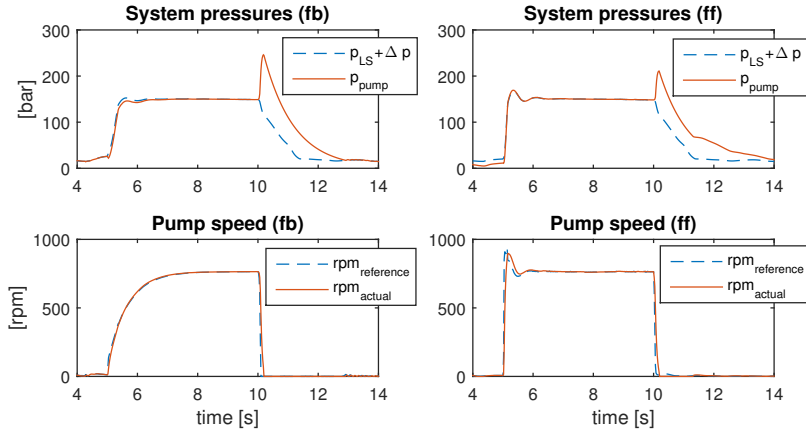


Figure 6.9: Step responses of the feedback controller (left) and the feed forward controller (right) during a step of 0-100 % at 5.0 s and 100-0 % at 10.0 s.

6.2.2 Reference following

Step responses

A basic (and perhaps the most intuitive) way of determining the performance of a controller is the step response test. A step in valve position of the valve controlling the first boom is made from 0 % to 100 % and a while later a second step from 100 % to 0 % is made.

As seen in Figure 6.9, using feedback control the system pressure p_{pump} reacts quickly to the new LS-pressure p_{LS} , allowing the crane to move. However, it takes as much as two seconds for the pump speed to rise to its final value, rendering the initial movement of the crane very slow.

At the negative step there is a quite large peak in pressure, due to the valve quickly shutting off the flow, before the pump speed gets down to zero.

Also seen in Figure 6.9, the feed forward controller shows a much quicker response in pump speed, rendering the crane much more responsive. On the other hand, both the pressures and the speed display an overshoot, this is due to a model error in the estimation of required flow. The complementary pressure feedback controller compensates for this and the pressures and the flow return to a constant, stable value.

At the negative step the peak in pressure is significantly smaller than that of the previous case, thanks to the feed forward controller's more responsive behavior.

When looking at the response of a step from 0 % to 50 % and later back to 0 % the feedback controller (see Figure 6.10) shows a behavior much similar to the 0-100 % step. Note that the pump speed doesn't approach a value 50 % of the previous value. This is due to the pre-designed, nonlinear flow curve of the

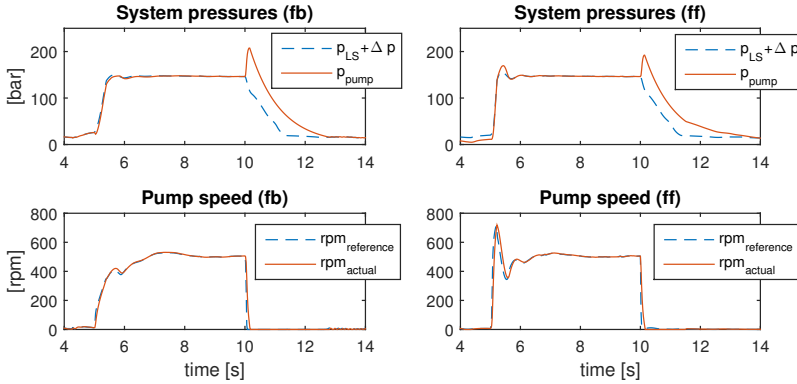


Figure 6.10: Step responses of the feedback controller (left) and the feed forward controller (right) during a step of 0-50 % at 5.0 s and 50-0 % at 10.0 s.

valves.

The feed forward controller displays a slightly worse step response, compared to the 0-100 % step response. It is clear that the adaptive parameter set (described in Section 5.2.2) which is used for calculating the required flow is not able to capture the nonlinear behavior of the valves fully. Nevertheless, the complementary pressure feedback controller is able to compensate for the model error and reach steady state.

When a step is made to a valve position that is less than fully open it is also interesting to study the response from the true flow control. The response of a step from 0 % to 50 % and later back to 0 % with true flow control can be seen in Figure 6.11. The initial part of the response is the same as for the feed forward since true flow control is not activated until the operator signal has been set for some time. The valve starts opening more than what the original operator signal corresponds to 1.5 s after the step has been made, see the degree-of-activation in Figure 6.12. At this point, the pump speed starts to increase, following the increase in valve opening. When the flow through the valve corresponds to the required flow from the feed forward the pump speed settles on a level even though the valve opening continues to open. As the valve continues to open and the flow is constant the pump pressure starts to decrease and does not follow the LS-pressure any longer. About 5 s after the step has been made the valve is fully opened and the true flow control is completely activated. Both the pump pressure and the pump speed are now settled on stationary levels. Note that the stationary level of the speed differs from the level obtained with ordinary flow feed forward due to model errors that the complementary feedback no longer takes care off when true flow control is activated. The true flow control is deactivated about 1 s after the step 50 - 0 % has been made since the function is no longer the heaviest load.

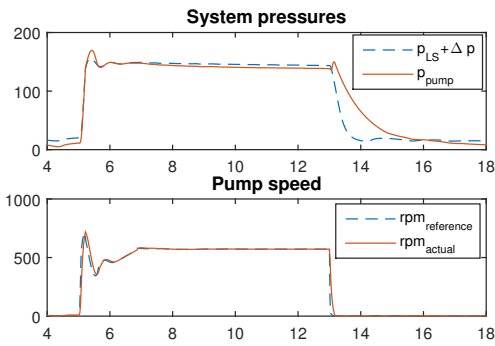


Figure 6.11: Step responses of the true flow controller during a step 0-50 % at 5.0 s and 50-0 % at 13.0 s.

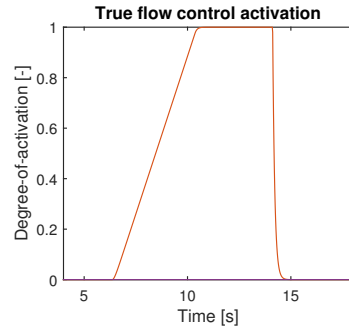


Figure 6.12: Degree-of-activation of the true flow control during a step 0-50 % at 5.0 s and 50-0 % at 13.0 s.

Positions in drive cycle

Another way of evaluating the performance of the controllers is to analyze how well the crane is able to follow a pre-defined drive cycle.

The drive cycle reference angles can be seen topmost in Figure 6.13. How well the crane is following the drive cycle is presented in the second and third graphs of the figure, where the differences between actual and reference angles are plotted for the feedback controller, the feed forward controller and the true flow control. As can be seen in the figure, the deviations are quite large for the true flow control, this is due to the modeling error not handled by the adaptive parameter set.

For the feedback and feed forward controllers, the largest deviations occur during changes in angular speed.

6.2.3 Speed

To define how fast a controller is, both the time to complete a drive cycle realized by operator signals and the response time to a step in the operator signals are interesting to investigate. The time for the different controllers to complete the drive cycle can be found in Table 6.2.

Strategy	Time [s]
Pressure feedback	75.80
Flow feed forward	74.46
True flow control	78.62

Table 6.2: Time to complete drive cycle for the different controllers.

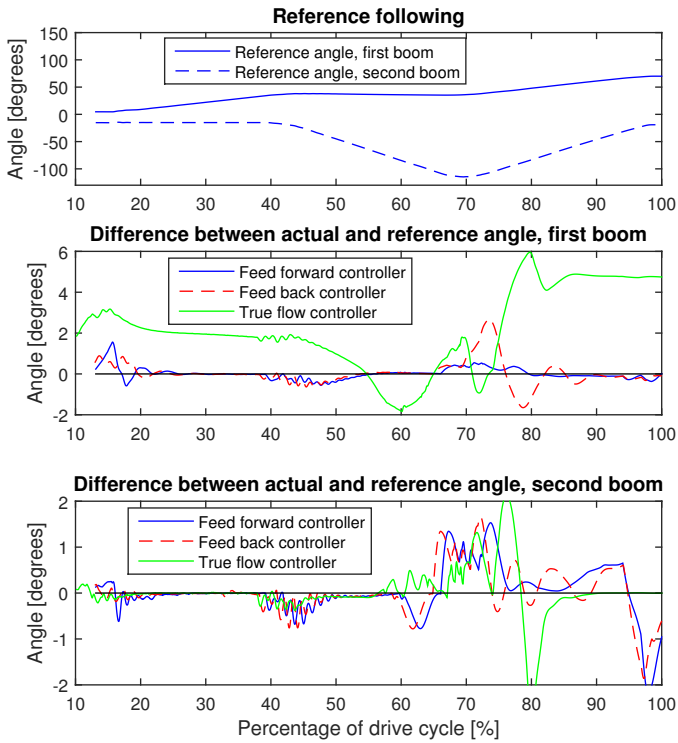


Figure 6.13: Reference following of the crane. The upper graph shows the drive cycle angles. The middle and lower graph shows the difference between actual and reference angles when the drive cycle is run with the feed-back controller, the feed forward controller and the true flow controller. The runs have been scaled time-wise due to the different completion time of their respective runs.

As can be seen on the left side of Figure 6.9 the rise time for the pump speed from a step in the operator signal from 0-100 % (for the first boom) is approximately 2 s when using pressure feedback control. When using the flow feed forward the rise time is only about 0.1 s, see right side of Figure 6.9. A fast step response in pump speed means that the crane function gets the desired flow and thereby starts moving with the desired speed quickly.

The time for the system pressure to settle is about 2 s for the pressure feedback and 1.5 s for the flow feed forward according to the previously mentioned figures. If the pump pressure overshoots the LS-pressure before settling, unnecessary energy losses occur.

The initial response of the true flow controller is identical to that of the flow feed forward since the true flow control is not activated until the function has been used for a certain period of time.

6.2.4 Oscillative behavior

The controllers described in previous sections have been tuned to primarily feature a very good robustness and secondly as fast as possible responsiveness.

During simulations of different drive cycles, step responses of different magnitudes etc, the controllers show very little or no tendencies of oscillative behavior. If the controllers would be tuned to show faster responses the robustness lowers and the risks of oscillative behavior increases. The oscillations can occur in several forms, magnitudes and frequencies, some examples are:

- Oscillations due to the inverter not being able to realize the signals from the controller fast enough. These oscillations are more probable during fast events or high pressures (power limitations). These oscillations are typically in the frequency range of 10-20 Hz.
- Oscillations due to low dampening of the crane. These oscillations are caused by the crane, which is a quite under damped system. These oscillations are typically in the range of 0.5-3 Hz depending on the distance to the center of gravity of the crane.

A discussion regarding the problems of oscillations can be found in Section 8.3.3.

6.2.5 Robustness

Since the system is highly nonlinear and a mathematical description of it is hard to define, see Section 5.5, the robustness of the controllers is investigated by simulations of the reference drive cycle.

First, a model error is introduced in the controller by changing the value of the displacement of the pump. Neither the pressure feedback nor the flow feed forward have any problems performing the drive cycle with a good cycle time and energy consumption when having a large model error, they show no tendency of not managing the drive cycle for values of the displacement between 1/2 to 2

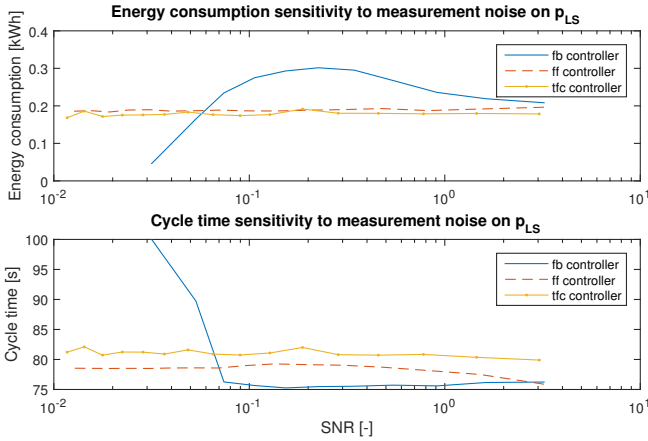


Figure 6.14: Comparison of energy consumption (upper) and cycle time (lower) sensitivity to measurement noise on p_{LS} . The feedback controller seem to be most affected by this type of noise, being unable to complete the drive cycle when there is too much noise.

times the correct value. A larger model error than the half or the double size of the correct value is not considered to be plausible.

The true flow control, that does not have the help of a feedback when fully activated, suffers more from model errors than the other controllers. It can manage the drive cycle with the value of the displacement between 50 to 200 % of the correct value but for larger deviations the movements of the crane become so slow/oscillative that it does not complete the drive cycle in time.

Secondly, measurement noise is added to the measurements of the LS-pressure and the pump pressure. In Figures 6.14 and 6.15 the energy consumption and the cycle time are displayed as function of the signal-to-noise-ratio (SNR) for the LS-pressure and the pump pressure respectively.

None of the controllers show any sign of being much affected, with regards to the cycle time, by noise down to an SNR of the LS-pressure of about 0.1. However, at an SNR of 0.03 the cycle time of the feedback controller is 100 s. This is the limit of simulation time set during simulations and the simulation was thus stopped before the crane had completed the drive cycle. The energy consumption for this point should be discarded since the drive cycle wasn't completed.

As to energy consumption, the flow feed forward and the true flow control show no sign of being affected by the noise. The pressure feedback starts to be affected at an SNR of about 1.

Similar to the behavior with noise on the LS-pressure, the energy consumption of the pressure feedback starts to rise at an SNR of about 1-2 for the pump pressure. The feed forward and the true flow control are somewhat affected below an SNR of about 0.4.

The cycle time sensitivity to noise on the pump pressure is most significant for the feed forward controller.

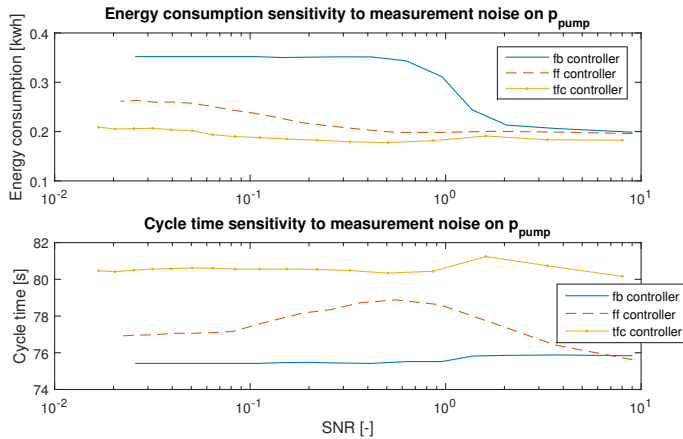


Figure 6.15: Comparison of energy consumption (upper) and cycle time (lower) sensitivity to measurement noise on p_{pump} . The feedback controller seems to be most affected by this type of noise with regards to energy consumption and the feed forward is a little bit more affected with regards to cycle time than the other two.

6.2.6 Performance of the adaptive parameter set

The adaptive parameter set controller block, described in Section 5.2.2, is created with the aim of adjusting the parameters to a "good average" where many previous situations play a part. The set up/tuning of the parameter set is done by simulating the crane over a long time (several hours), while performing a large number of random movements. This way most of the valve positions are affected and the corresponding parameters thereby get tuned in.

Figure 6.16 shows the values of the different parameter sets for the functions first boom, second boom and extender respectively during 10'000 seconds simulating random drive cycles. The set for the crane rotation at the base is omitted due to operator control problems, see the discussion in Section 5.4. As seen in the figure, some parameters don't settle completely at a specific value during the random drive cycles, but they do end up in the vicinity of a certain value. Figure 6.17 shows the original values of the parameter sets together with the values achieved after tuning. The values are later used to calculate the hydraulic flow required of the pump, at different valve positions (i. e. operator commands).

When the parameter set has been tuned in, it is apparent during simulations that the signal of the complementary feedback controller is centered on the value one (note that this value is multiplied with the feed forward signal, hence the value "one" is the equilibrium), but *only when looking over a fairly large period of time*. When inspecting shorter time periods it becomes apparent that the feedback controller signal is *not* constantly at the value one, see Figure 6.18, but can be quite a bit away from this level. A non-one value indicates that the feedback controller has to adjust the feed forward signal. This suggests that there are other

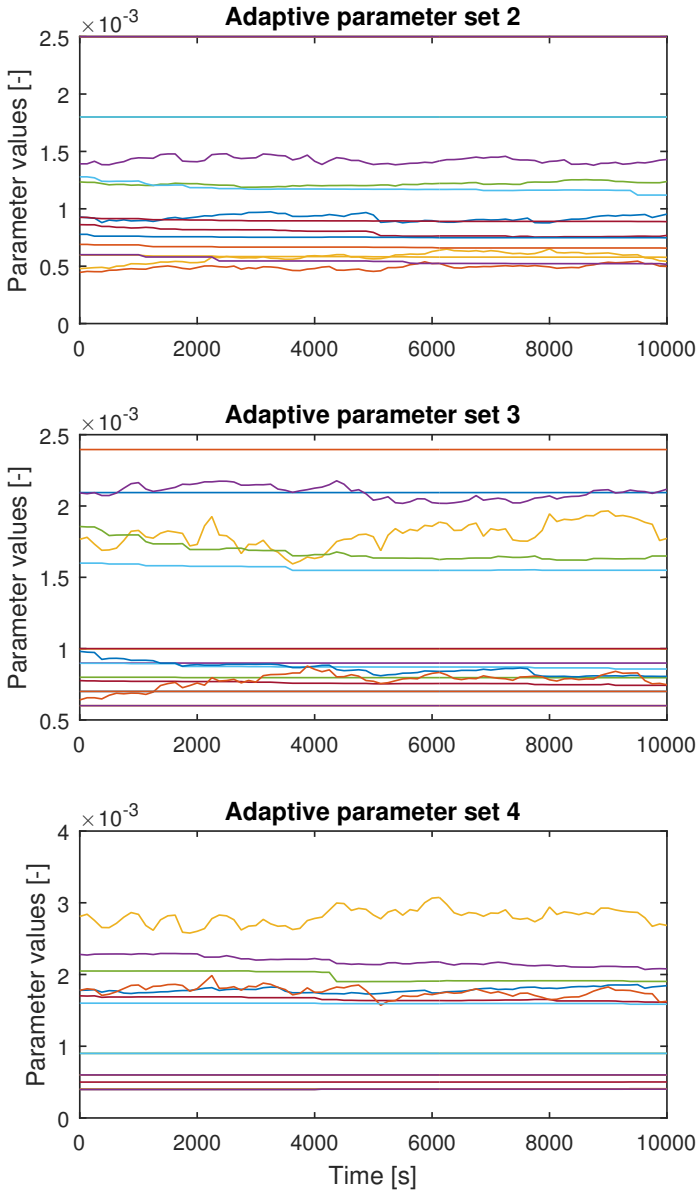


Figure 6.16: The parameter values of the adaptive parameter sets, during a long simulation time with the crane performing random movements. The parameter values aren't constant, but remains in the vicinity of a certain value over time. Note that parameter set 1 is omitted due to the control problems mentioned in the discussion chapter.

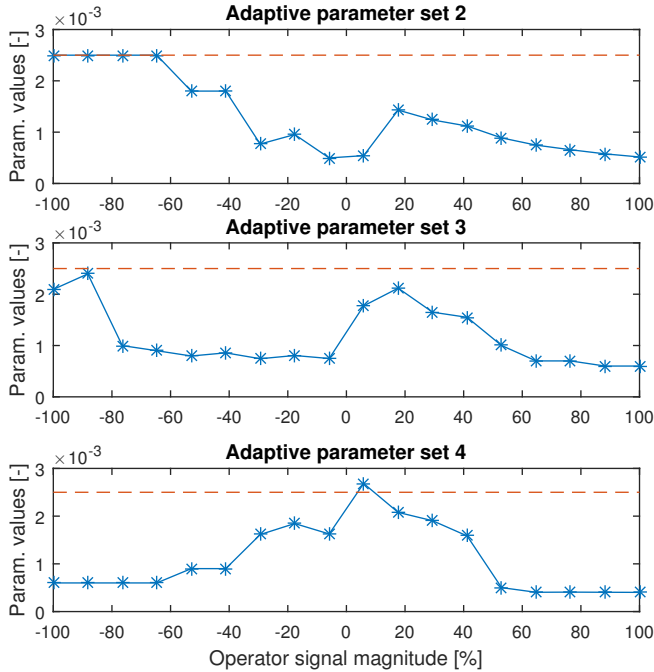


Figure 6.17: The adaptive parameter sets (i. e. the parameters corresponding to different operator magnitudes). The dashed lines represent the start values from before tuning has begun and the solid lines the values achieved after tuning. Note that the tuned values vary significantly, indicating that the flow characteristics of the valves are highly non-linear.

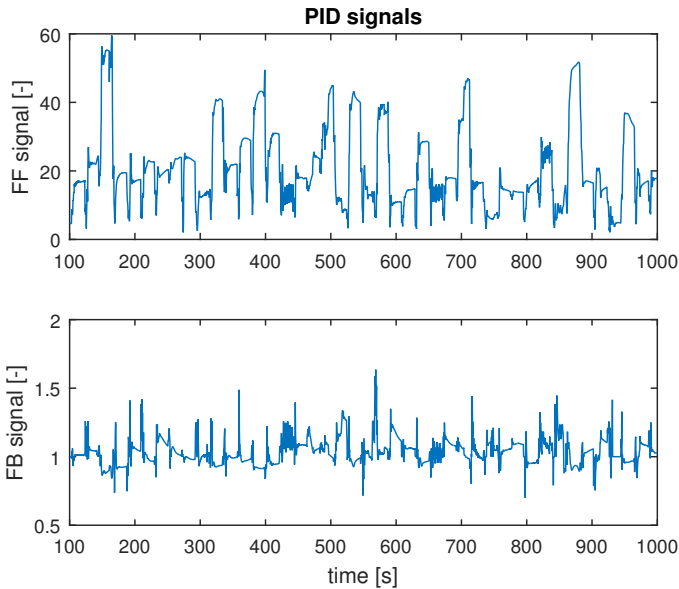


Figure 6.18: The output from the feed forward controller (top) and the complementary feedback controller (bottom). Note that the feedback signal is centered around a value of one, which indicates that the adaptive parameter set is properly tuned.

phenomena that play a part in the resulting flow through the valves, besides the operator signal-valve position relationship portrayed by the adaptive parameter set.

Even though the adaptive parameter set does not manage to perfectly adjust the feed forward model both the flow feed forward controller and the true flow controller show better performance when using the tuned parameter values compared to using the original values. The problems of using an incorrect flow model are described in Section 2.1.4.

7

Energy study

In this chapter the energy losses in the different components of the power pack is presented, compared and discussed. Data to the study is obtained from simulations of a reference drive cycle in the Simulink model using the selected feed forward controller. The results from this study can be used to indicate where improvements can be made to decrease the total energy consumption of the system. Another purpose with this study is to investigate if the size and working area of the components are matched to the operating points of the drive cycle, with regards to energy efficiency. This is discussed for each component of the power pack.

7.1 Battery

As can be seen in Figure 4.9 the internal resistance of the battery gives rise to a large voltage drop over the battery for high currents, causing large energy losses. In the model, the internal resistance is modeled as a constant and thus the efficiency of the battery decreases linearly with increasing current and also with increasing input power since $P_{in} = U_{oc}I$ and $U_{oc} = constant$. The efficiency of the battery during the drive cycle is displayed in Figure 7.1 together with the input power as a reference. It is clear that the difference between the efficiencies at low power inputs, $> 90\%$, and at high power inputs, down to 70% , is large. To increase the efficiency at high power a battery with a lower internal resistance would be needed.

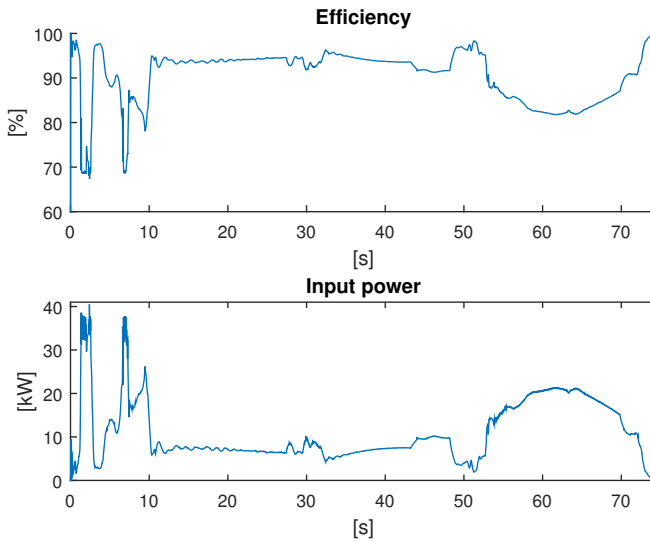


Figure 7.1: Efficiency of the battery (upper) and input power to the battery (lower) during the drive cycle.

7.2 Inverter

The losses in the inverter can be divided in switching losses (constant) and conduction losses (proportional to electric current squared). A simplification of this is to view the efficiency as constant, which is accurate enough for loads over approximately 20 % of rated power. Below this point, the low conduction losses do not cancel out the impact of the switching losses and the efficiency drops.

In Figure 7.2, the power drawn from the inverter is plotted, along with marker lines for rated power and 20 % of rated power. As can be seen in the figure, the power is above 20 % for a majority of time, by which a conclusion can be drawn that the simplification of using a constant efficiency value is justified. This constant efficiency is implemented in the Simulink model.

It can also be noted that the power rarely overshoots the rated power, indicating that the inverter size is adequately matched to the application.

7.3 Electric motor

The figure 7.3 shows the operating points from the drive cycle simulated on the model marked on the efficiency map obtained from the measurement points provided by the operator. When studying the operating points it becomes clear that the motor is operated in a broad range of speeds. A large part of the time the motor is operated at lower speeds than rated and the efficiency of the motor unfortunately drops fast below 1000 rpm (the efficiency for the operating points

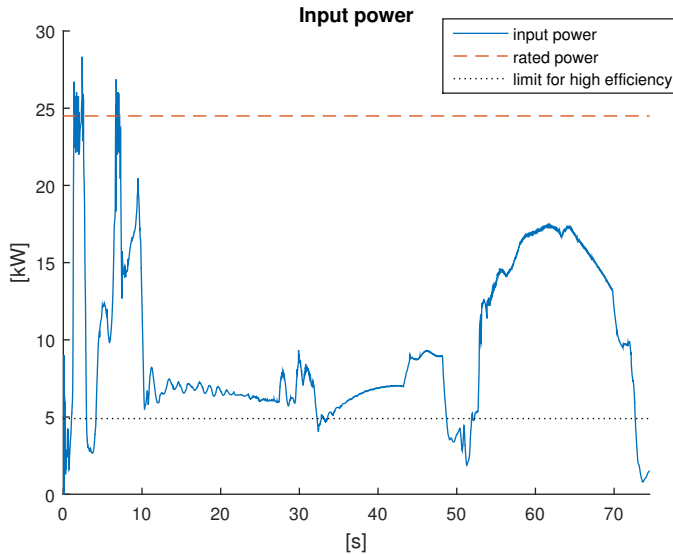


Figure 7.2: *Input power to the inverter during the drive cycle, with marked rated power and lower limit for high efficiency. The input power lies mainly between the two limits, which means the efficiency of the inverter can be simplified as a constant.*

outside the efficiency map can be assumed to be low by comparing the map to other known efficiency maps, see for example Burwell's article [Burwell, 2013]). To increase the efficiency of the motor part of the system, during a typical drive cycle for a crane, a motor with a broader region of high efficiency below rated speed would be preferable. According to the investigation in Appendix C a synchronous motor could be a better alternative with respect to this than the asynchronous motor currently used.

7.4 Hydraulic pump

The efficiency map of the hydraulic pump can be seen in Figure 7.4. The efficiency of the hydraulic pump is a combination of a hydro-mechanical efficiency and a volumetric efficiency. The hydro-mechanical efficiency is related to friction and pressure losses, whereas the volumetric efficiency is related to "internal leaks" and flow losses. It should be noted that the data points used for creating the efficiency map is (unfortunately) only placed in the region $T=[50-250]$, the efficiency map outside this region is therefore extrapolated and the accuracy might suffer.

In the Figure 7.4, the operating points of the drive cycle are also plotted on the efficiency map. The size of the pump, i. e. the displacement of the pump, seems to be reasonably well adapted to the operating points displayed. A larger

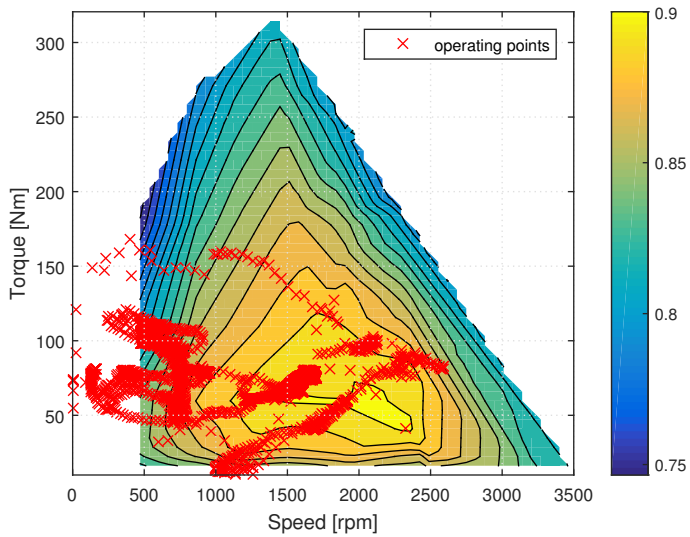


Figure 7.3: Operating points of the electrical motor during a simulation of the drive cycle, on top of efficiency map derived from measurement data. Note that the motor during simulations is operated outside the area of measurement points a large amount of the time. The physical motor is able to run outside the measured area but it's efficiency is low, indicating that it is not perfectly fitted to the working area of the system.

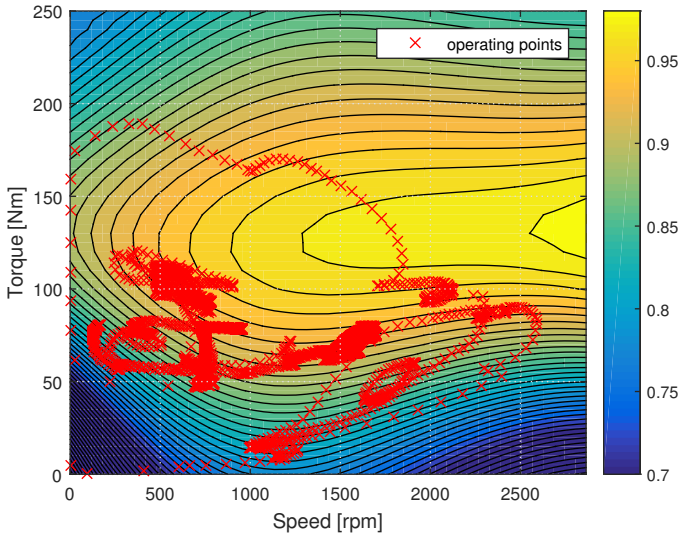


Figure 7.4: Efficiency map of the hydraulic pump derived from manufacturer data. Red crosses are operating points from simulation of the drive cycle

pump would have the operating points displaced towards the upper-left of the graph, which might render a better efficiency, but due to a maximum torque limit of the electric motor, this area might be unreachable for the system.

It is worth noting that the hydraulic pump is a general-purpose pump, not specifically adapted to the operating points common of this application.

7.5 Comparison

In Table 7.1 the energy losses for the different components during a drive cycle are presented. In Figure 7.5 the power losses of the different components during the drive cycle are displayed together with the useful power output from the power pack. It is clear that the battery and the electric motor give rise to the highest losses and that improvements in their efficiencies would have a large impact on the total losses. To improve the efficiency of the battery the lead-acid battery could be switched to a lithium-ion battery with a significantly lower internal resistance. The efficiency of the motor could be improved by switching to a synchronous motor or a motor with a rated power better matching that of the inverter.

Component	Energy loss [kWh]	Part of total losses [%]
Battery	0.0296	35.8
Inverter	0.0039	4.7
Electric motor	0.0307	37.1
Hydraulic pump	0.0184	22.2
Total losses in power pack	0.0827	-
Total energy consumption	0.2265	-

Table 7.1: Energy losses for the different components of the power pack

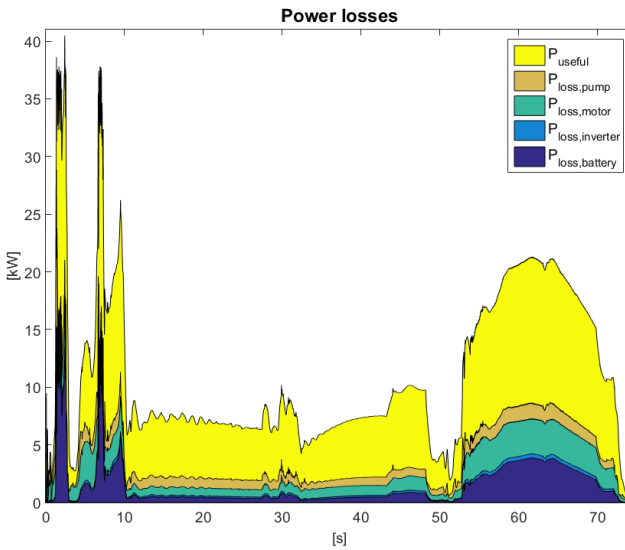


Figure 7.5: Comparison of power losses of the different components during the drive cycle. The battery and motor are dominating the losses.

8

Comparison and analysis

8.1 Test rig

As can be seen in Figure 8.1 the efficiency of the system with a variable speed pump (configuration 2) is significantly higher than that of the system with the variable displacement pump (configuration 1) in the sections with low power output. This is due to the losses from the constant high rotational speed of the variable pump of configuration 1 compared to the low speeds of the fixed pump when a low power is required. However, since the power in these sections is low, the absolute energy losses are not that significant. The power lost is better visualized in Figure 8.2 where it can be seen that the accumulated losses during the cycle increase almost linearly for both configurations and that the difference at the end of the cycle is significant. It is also clear that the system with configuration 1 performs better with a fixed speed of 2000 rpm than 2500 rpm, mostly due to a higher efficiency in the sections with low power output for the same reason as mentioned above.

During the drive cycle the best system ($n = 2000$ rpm) with configuration 1 has produced 0.59 kWh of useful energy and 0.60 kWh of energy losses. The corresponding values, calculated as a mean of the two test results, for the system with configuration 2 is 0.56 kWh and 0.40 kWh. This gives a total efficiency of 49 % for the system with configuration 1 and 59 % for the system with configuration 2. This result supports the conclusion that configuration 2 is an energy efficient configuration from the study of previous work in the area, see Section 1.3. It should be noted that there is an uncertainty to these efficiencies due to the inaccuracy of the measuring instruments. However, although the absolute values of the efficiencies might be slightly off, the relative difference between them is deemed to be accurate.

As described in Section 3.2, the system was not able to provide enough power

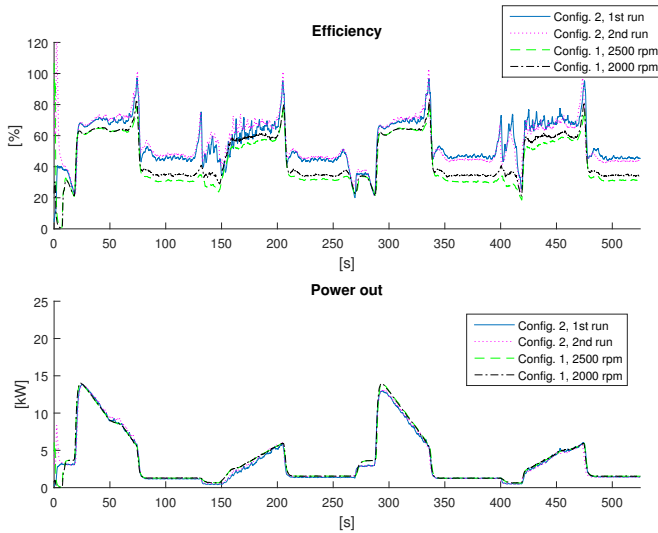


Figure 8.1: Calculated efficiencies and output power during the different runs of the test rig. Config. 2 (the variable speed pump) show higher energy efficiency than Config. 1 (the fixed speed pump), especially during low power output.

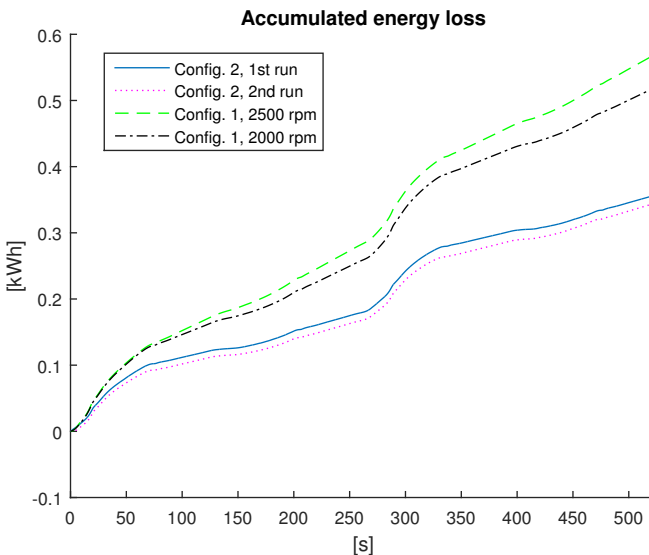


Figure 8.2: Accumulated energy losses during the different runs of the test rig. Config. 2 (the variable speed pump) has significantly lower energy losses than Config. 1 (the fixed speed pump).

to follow the original drive cycle, mostly due to the high internal resistance of the battery. A way to deal with this problem would be to replace the lead-acid battery with a lithium-ion battery that has a significantly lower internal resistance and a higher power density. To manage the drive cycle, the battery must be able to provide 81 kW if the efficiency of the system is 70 % at high loads. The inverter and the electric motor will also have to be replaced in order to be able to produce the required power.

The question of controllability will be mainly answered by the results from the simulations. However during the parameter tuning of the physical test rig it became apparent that the pressure feedback controller has large tendencies of oscillative behavior, especially at lower speeds. This behavior is thought to be mainly due to control signal delay in the controller-inverter-motor chain.

As to the cost of investing in and running the electric-hydraulic application it can be assumed that the motor and the inverter can be the same for both configurations. A fixed pump is somewhat less expensive than a variable one but the majority of the investment can probably be saved in the battery. A 20 % higher efficiency for configuration 2 gives the opportunity of downsizing the battery with 20 % compared to configuration 1 while keeping the output capacity constant. If a lithium-ion battery with a capacity of 40 kWh would be suitable for the least efficient configuration, the capacity needed for the more efficient configuration would be 8 kWh less. With a price estimate of €600/kWh (see the theory about battery packs in Appendix B) the savings would be €4800. The use of a battery with less capacity also means a lighter additional weight to the truck and the possibility of a heavier load during operation.

8.1.1 Comparison with combustion engine driven system

It is also interesting to compare the electric driven system (both configuration 1 and 2) with the conventional combustion engine driven system dominating the market today. Two obvious advantages with an electric driven system is the lack of exhaust emissions and the low sound level during operation. This allows for operation in new environments, for example indoors or at night.

A significant drawback of the electric-hydraulic system is the additional investment cost and weight of the battery, inverter and electric motor. The return of investment time for the electric system is calculated in Appendix D to be approximately 5 years, although this number largely depends on how much and how hard the crane is operated. The currently falling lithium-ion battery prices indicate that the return of investment time will be shorter in the future, making the concept an interesting technology to further develop.

8.1.2 Environmental impact during product life-cycle

In this section the impact on the environment of the system with configuration 2 during the different stages of its life-cycle will be briefly discussed. The battery is assumed to be a lithium-ion battery and the motor is assumed to be an induction motor.

Manufacturing

Three additional components, battery, inverter and electric motor, are required by the electrically driven system compared to a conventional diesel driven system. The manufacturing of these components requires raw material and energy in different quantities. The mining of the metals required produce waste and might pollute the local environment.

Charging

The environmental impact of charging the battery depends on the energy source used to produce the electricity. An average value that can be used is the emission value of the Nordic electricity mix, since most of the electricity in Sweden is bought at the Nordic trade market Nord Pool. According to Energimyndigheten [Ene], the average value of the emissions from the Nordic electricity mix was 125.5 g CO₂ equivalents/kWh during the period 2005-2009. This can be compared with the emissions from diesel fuel which is 263.7 g CO₂/kWh.

Operation

The system has no emissions during operation and can thus be operated in urban areas where pollution of the local environment is undesirable.

Recycling

The metals of lithium-ion batteries can be recycled but since the availability of the raw materials is high, see Appendix B, and the batteries are not considered as hazardous waste there is currently no large economical gain in doing so. According to a company that runs a pilot plant for the recycling of lithium-ion batteries, based in Hofors, Sweden [Hållén, 2009], 95 % of the metals (that make up 1/3 of the total weight of the battery) can be recycled. Another 1/3 of the material can be energy recycled.

8.2 Simulation model

The model used for simulation of the system was created with the purpose of evaluating the controllers in mind. Due to the extensiveness of the model (including battery, inverter, electric motor, hydraulic pump, hydraulic system and mechanical crane model), to validate all parts of the model was deemed to be beyond the scope of this thesis.

The parts most important for the energy study (the battery and the electric motor) was modeled and validated by measured data and are considered to be reasonably accurate. The other parts in the model have *not* been validated to measured data but have been constructed with best practice in mind.

As a consequence, the absolute values of the results from simulations should not be used independently. However, they can be used for comparisons between

different simulation runs to draw conclusions about general trends and behaviors.

8.3 Simulated controllers

The first conclusion that can be drawn from the results in Section 6.2 is that all three proposed controller perform well with respect to the criteria investigated. It is impossible to determine which controller performs best in all possible situations. In the following sections the pros and cons of the different controllers will be discussed.

8.3.1 Energy efficiency

The energy consumption is almost equal for the pressure feedback and the flow feed forward. The slightly higher energy consumption for the feed forward is probably due to controller-model errors making the controller initially outputting a too high flow before the complementary feedback adjusts the flow to a correct value.

The true flow control concept shows a promising increase in energy efficiency, thanks to is being able to cut pressure losses in the hydraulic system.

8.3.2 Discussion about speed

The difference between the pressure feedback and the flow feed forward controller in regards to completing the drive cycle is quite small, 74.4 versus 75.8 seconds. However, these values is (unfortunately) very dependent on the operator controller, which renders the completion time of the drive cycle not a good measurement of controller performance.

The true flow controller is somewhat slower than the other two (78.6 s in the drive cycle), but this is due to the system being harder to control for the operator and not a fault of the controller.

If instead analyzing a step response, the feed forward controller shows a much faster response than the pressure feedback controller, 0.2 versus 2 seconds. This kind of behavior is important to the end-user-performance, since a real crane operator often operates the crane with joystick movements similar to steps.

The true flow controller showcases the same responsiveness as the flow feed forward controller due to the nature of its delayed activation.

8.3.3 Discussion about robustness

Parameter tuning: The PI-parameters were tuned to a point where a good robustness could be shown and the controllers responsiveness was as good as possible. Several parameter sets with values ranging around this point where then tested with regards to robustness and performance. It can be concluded that the systems are not very sensitive to the exact values of the parameters.

Oscillations: As previously mentioned, the controllers were tuned to a point where no or little oscillations are present. When sped up however, the controllers showed different degrees of oscillating behaviors. Especially the pressure feedback controller shows a rather oscillative behavior when tuned too aggressively, especially at very low speeds. This is due to a signal delay in the inverter/electric motor, much like in the real hydraulic test rig. The nonlinearity of the pump only being able to operate in the forward direction is also contributing to the oscillations at very low speeds.

Model errors: Both the stand alone pressure feedback controller and the one with complementary feedback controller seem to handle model errors very well since the controllers manage to complete the drive cycle with a model error of over 100 %. The true flow controller is however completely dependent on the model when activated, which makes its performance directly proportional to the model error.

Measurement noise: All controllers handle measurement noise very well, a signal-to-noise-ratio of 10 % causes no big problems to the ability to perform the drive cycle, as long as the noise is centered around zero. The main reason for this behavior is the low pass nature of the controllers together with the inverter and electric motor.

8.4 Discussion about methods

In retrospective view, there are several things that could have been done differently during this project. Listed below are some of the biggest possibilities of improvement:

- During the measurements of the test rig, some of the instruments used were not calibrated. It would have been good to calibrate the instruments prior to the measurements and thus have been able to calculate a confidence interval of the results.
- During the modeling of the crane, the model of the hydraulic system was made in Hopsan using standard hydraulic components. In retrospect, a validated model of the hydraulic system might have provided a better environment in which to evaluate the controllers, handle realistic system behaviors and develop well functioning control strategies.
- If the inverter and the motor had been modeled as three-phase-models, the transient behavior of the system would probably have been more accurate and well motivated.
- The operator controller used for creating a repeatable drive cycle could have been better modeled with regards to the behavior of a real operator. This would have resulted in a better environment for evaluating the performance of the controllers.
- The method for comparing different controllers was hard to define. It was difficult to weight different criteria against each other and to sum them to an overall impression.

9

Conclusions

9.1 Conclusions from this thesis

The final conclusion of this thesis is that there are benefits to be gained in terms of energy efficiency by controlling the speed of a fixed displacement hydraulic pump, compared to using a fixed-speed variable displacement pump.

The three investigated strategies to control the pump speed are each characterized by different advantages and drawbacks:

- The basic pressure feedback controller shows a decent performance and requires little modification to the crane controller system.
- The flow feed forward controller shows great performance but requires a good flow model and some implementations in the crane controller system.
- The "true flow control" concept shows an increased energy efficiency compared to the other two, but is more sensitive to flow model errors and requires the individual load pressures to be measured.

9.2 Future work

The area of energy-efficient hydraulics is a rather young area of study and there are a lot of things to further investigate.

Some interesting concepts that have arisen during the work on this thesis are:

- Examining the concept of pressure feedback torque control, ignoring the speed of the electric motor and only focusing on the relationship between electric current, torque and hydraulic pressure.

- Further analysis of an adaptive parameter set as an alternative to an actual observer. Perhaps, by utilizing a multidimensional matrix of parameters the flow can be properly estimated?
- Examining the hydraulic concept of using two separate pressure rails, one for high pressures and one for low pressures, further minimizing pressure losses in the system.
- Examining the concept of a variable-speed, variable-displacement hydraulic pump. With two degrees of freedom the controllability and energy efficiency might be increased further, since the operating point then can be arbitrarily selected and optimized with regards to efficiency maps of both motor and pump.

Appendix

A

Selection of controllers

This appendix chapter describes the process of selecting the best controllers from different controller strategies.

A.1 Method for selecting controllers

To be able to compare controllers from different controller strategies with each other, the selected controllers should represent the best possible behavior of their respective strategies. The representative controllers were selected using the following steps:

- **Step 1:** Good P and I values of the PI-feedback controllers were selected by investigating step responses for the three active functions. A D-part was also added to the controllers initially but did only increase the tendency of oscillations so it was discarded during the rest of the investigation.
- **Step 2:** A range of P and I values, ranging around the above selected values, were selected. A drive cycle simulation was run for each combination of values in the range.
- **Step 3:** The overall performance of the controllers with respect to the following performance factors (see Section A.2 for calculation of the factors) from the drive cycle simulation were investigated:
 - energy consumption, E_{tot}
 - cycle time
 - oscillativity(p_{LS})
 - oscillativity(p_{pump})

- oscillativity(first boom angle)
 - oscillativity(second boom angle)
 - oscillativity(extender angle)
 - referenceFollowing(rpm_{ref} , rpm_{act})
 - referenceFollowing(p_{LS} , p_{pump})
- **Step 4:** A smaller number of controllers ranging from the best to the worst performing were selected for further investigation.
 - **Step 5:** A robustness test was performed on each of the selected controllers. The overall performance of the controllers with respect to the same factors as above was investigated. The following signals were perturbed:
 - Pump displacement (model parameter used in controller)
 - p_{LS} measurement
 - p_{pump} measurement
 - Valve position signal from operator
 - Weight of the load
 - **Step 6:** The best candidate was simulated again, without disturbances, and signals were plotted and investigated to make sure that the numbers representing the performance factors were a good indication of the behavior of the system.
 - **Step 7:** The best candidate was tested on the same step responses as in step 1 to make sure that everything looked okay.

A.2 Calculation of performance factors

$$E_{tot} = \sum \Delta P \Delta t \quad (\text{A.1})$$

$$oscillativity(signal) = \frac{\sum \frac{|signal - signal_{lowpass}|}{\text{mean}(|signal|, |signal_{lowpass}|)}}{\#samples} \quad (\text{A.2})$$

$$referenceFollowing(signal_{ref}, signal_{act}) = \frac{\sum \frac{|signal_{ref} - signal_{act}|}{\text{mean}(|signal_{ref}|, |signal_{act}|)}}{\#samples} \quad (\text{A.3})$$

B

Discussion about different types of battery packs

The battery pack providing the system with energy is a large cost relative to the whole system, if the system would evolve to a product the selection of the battery would be important. Several aspects must be then considered:

- Storage capacity
- Maximum power output
- Efficiency
- Weight
- Material
- Life cycle cost
- Life span (number of charge cycles until performance is considerably reduced)
- Memory effect (loss of storage capacity due to partial discharge/charge)
- Environmental impact

The current battery pack of the test bench consists of lead acid batteries. Other common rechargeable battery types are lithium-ion, nickel-cadmium (NiCd) and nickel metal hydride (NiMH). Table B.1 lists some characteristics of these batteries.

Battery	Advantage	Disadvantage
lead acid	lowest cost	lowest energy density
NiCd	best rechargeable cycle life	memory effect, cadmium is toxic
NiMH	high energy density	-
lithium-ion	high energy density	expensive

Table B.1: Characteristics of common batteries, [Encyclopaedia-Britannica, 2015]

A comparison between lead acid and lithium-ion batteries is done in an article in the e-magazine AltEnergy [Albright et al., 2012]. The comparison shows that to get the same life span in terms of cycles the lead acid can only be discharged to a depth of 30 % while the lithium-ion (LiNCM) can be discharged to a depth of 80%. This means that to get the same life span the lead acid has to have 2.5 times more storage capacity than the lithium-ion. The cost of purchase for the lead acid is said to be \$120/kWh and for the lithium-ion \$600/kWh. If only the life span together with storage capacity are considered the lead acid will be the least expensive alternative. The NiMH has about the same cycle life as the lead-acid and the cost of purchase is somewhere between lead-acid and lithium-ion [Linden and Reddy, 2006]. Price estimates of different batteries from a paper about e-bikes [INSG and Stewart, 2014] are €30/kWh for lead-acid, €300/kWh for NiMH and €600/kWh for lithium-ion.

For a mobile application the weight of the battery could be important. The specific energy of a lead acid battery is 30-50 Wh/kg, the energy of the lithium-ion is 150-194 Wh/kg and for the Ni-MH it is 65-95 Wh/kg [Jha, 2012]. However, the impact of a battery of about a tonne on a large truck that is immobile during a large part of its working days might not be so big, but when transporting the maximum allowed load is decreased by a tonne which must be taken into consideration.

The battery's performance in high or low temperatures might also be of importance since the cranes are expected to be able to work outside the year around. The operating temperatures for discharge are pretty similar for different types of batteries: -20° to 60° for lead-acid, -20° to 65° for Ni-MH and -20° to 75° for lithium-ion [Jha, 2012]. A diagram from the article from AltEnergy [Albright et al., 2012] shows that at 33° the lead acid battery loses its capacity 50% faster (in terms of cycles) than at 25°. For the lithium-ion no difference can be seen. Further, while both types of batteries lose capacity at low temperatures the difference at -20° is significant, 80% capacity for lithium-ion and 30% for lead acid. Another study, [Pierozynski, 2011] shows that the same number for NiMH is 74%.

The article from AltEnergy [Albright et al., 2012] also discusses the environmental impacts of the two types. Since lead acid batteries have the lowest energy density they also require the most raw material per storage capacity. A large part of the lead acid batteries is however recycled but the recycling brings its own problems. Many batteries are recycled in development countries where the security measures are very low and people and the environment are being intoxicated [Hansson, 2014].

Element	Reserves [million tonnes]	Average production per year for 2013 and 2014 [million tonnes]
lead	87	5.49
lithium	13.5	0.036
nickel	81	2.5
copper	700	18.5
cobalt	7.2	0.115
nickel	0.57	0.018
aluminium	*	48.45
graphite	110	1.14

Table B.2: Availability of raw material.

* = "Sufficient to meet world demand for metal well into the future"

The lithium-ion battery consists of many different metals that could be harmful to the environment. In a study made by EPA [EPA and et al, 2013] three different cathode compositions for lithium-ion batteries are studied: $LiNi_{0.4}Co_{0.2}Mn_{0.4}CoO_2$, $LiFePO_4$ and $LiMnO_2$. The $LiNi_{0.4}Co_{0.2}Mn_{0.4}CoO_2$ was found to have the largest potential for environmental impacts, mostly due to the production and use of cobalt and nickel that are more toxic than manganese or iron.

Copper is another metal that can be found in lithium-ion batteries. According to the material supplier Targray [Targray, 2014], both the anode and the current collectors can contain copper. The active material of the anode is often graphite and the current collectors can also be made of aluminium.

As to the availability of raw materials, lead and copper are the elements with the smallest reserves in relation with the current production among the elements mentioned above according to the U.S. Geological Survey [USGS, 2015], see Table B.2.

The conclusion from this investigation is that lead-acid is probably the battery with the lowest life cycle cost. NiMH or lithium-ion can be considered as alternatives if light weight or small size lead to reduced costs. If the application is expected to be operated for long periods in low temperatures lithium-ion could be a good choice since it loses much less capacity in low temperature than the other types.

C

Discussion about different types of electrical motors

The electric motor used in this project wasn't specifically selected to match all of the requirements of the system. If the system would be commercialized in the future the motor would have to be selected according to some criteria:

- The motor has to be able to provide a torque higher than or equal to the highest torque required by the application, see Figure C.1.
- The efficiency should be high for a broad range of speeds since the motor will be operated at variable speeds.
- The price of the motor should be reasonable with respect to the current cost of the application.
- The motor should be easily controlled by a variable frequency drive (inverter).
- The power density of the motor should be high since any excess weight is undesirable in a mobile application.

According to Berkner [2008], who discusses the use of electrical to drive a hydraulic system, two types of motors dominate the market today, AC induction motors (asynchronous motors) and AC permanent-magnet motors (synchronous motors). For industrial applications the AC induction motor is the most common, or the AC synchronous motor for very large applications [Keyes and Eng, 2007]. A third motor type, the reluctance motor, is not very common today but could be in the future due to good torque-speed characteristics [Hashernnia and Asaei, 2008] and simple construction [DiRenzo, 2000]. Since the price of these motors is still high they will not be considered as an option in this project but could very well be an alternative in the future. The rest of this section will be a comparison

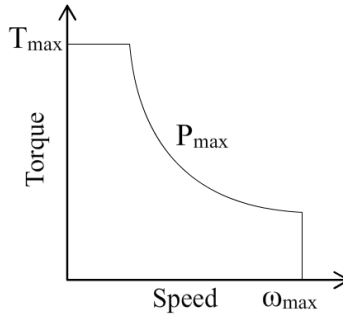


Figure C.1: The operating points of an electrical motor is typically limited by a maximum torque, speed and power.

between the induction motor and the permanent-magnet motor with focus on the above criteria.

The power density of a permanent-magnet motor is higher than that of an induction motor [Hashernnia and Asaei, 2008], [Burwell, 2013] and they are often more efficient [Keyes and Eng, 2007], [Burwell, 2013]. Burwell shows in his comparative study [Burwell, 2013] efficiency-speed diagrams for two comparative motors of 50 kW, one induction and one permanent-magnet. The motor used in this project will be of that magnitude, see Section 3.1, so the comparison is relevant. The weight of the induction motor in the study is 40 % higher than the permanent-magnet motor and the efficiency for the permanent-magnet is about 5% higher and high in a broader region both in speed and in torque than the induction motor. The main disadvantage of permanent-magnet motors is that they are more expensive than induction motors due to the large cost of the permanent magnet, Burwell's example of production costs is \$200 for the induction motor and \$260-540 for the permanent-magnet (large uncertainty due to volatile magnet prices). The volatile magnet prices are caused by the availability of the rare earth elements that the magnet consists of. However, one must also take into account increased battery cost for the induction motor to compensate for the lower efficiency. The study shows that for a certain desired battery capacity there will be a break even between the costs for the two motors. If the desired capacity is larger than that, the cost for the permanent-magnet system will be lower than for the induction motor system.

One way to deal with the weight problem of the induction motor could be to choose a motor rated for lower power than needed and then run the motor overloaded. Generally, motors can be overloaded for a short time without any damage but longer periods of overload can overheat the motor and reduce efficiency and life time.

A shortened life time however, is supposedly not a very big problem for the crane application of this project, since the life time of an electrical motor often is much longer than that of the crane.

As to controllability the speed of both the induction motor and the permanent-magnet motor can be controlled by an inverter as will be the case in this project. Since the permanent-magnet motor is synchronous, its mechanical speed is equal to its electrical speed which makes the control simple. No feedback is required as long as the motor does not drop out of synchronicity. The induction motor is asynchronous, i.e. the mechanical speed that needs to be controlled is not the same as the electrical speed that the inverter is connected to. The inverter can compensate for this with the use of a feedback loop. This means that the control system is a bit more complicated for the induction motor than for the permanent-magnet motor.

D

Cost comparison with a combustion engine driven application

In this appendix, the cost for investing in and running an electrical system is compared to that of a diesel driven system.

Three additional components are required for the electrical system; an inverter, an electric motor and a battery. The cost for the inverter and the motor is approximately 50'000 SEK although this sum may differ depending on the number of units bought. The price of a lithium-ion battery of 32 kWh would be € 19'200 (assuming a price of € 600/kWh) which is approximately 192'000 SEK. To calculate an approximate return of investment time for the electric system the cost of the electricity needed for charging the battery is assumed to be 0.8 SEK/kWh and the price of diesel fuel assumed to be 10.8 SEK/l (≈ 1.1 SEK/kWh). Further, a lithium-ion battery of 32 kWh is deemed to be sufficient for a normal day's work for an example crane. The number of working days per year is assumed to be 225, giving a total electricity consumption of 9000 kWh per year. A diesel driven crane of the same size consumes about 5500 l of diesel per year. This gives that the annual operation cost is approximately 7200 SEK for the electric system and approximately 59'400 SEK for the diesel driven system. With this annual saving of 52'200 SEK the return of investment time for the electrical system is about 5 years. It must be considered that the capacity of the battery will only last a certain number of discharges and that the battery might have to be replaced after some time to make sure that it lasts a whole work day. Depending on the type of lithium-ion battery the cycle life can range from 1000 - 3000 cycles, which means that the battery will have to be replaced every 4 - 13 years.

Bibliography

- Energimyndigheten - växthusgasberäkning. URL https://www.energimyndigheten.se/Foretag/hallbara_branslen/Hallbarhetskriterier/Fragor-och-svar-hbk/Vaxthusgasberakning/. Cited on page 78.
- Hopsan project. URL <https://www.iei.liu.se/flumes/system-simulation/hopsan?l=en>. Hydraulic and mechanics simulations, developed at LiU. Cited on page 26.
- Labview. URL <http://www.ni.com/labview/>. Cited on page 21.
- Albright, Edie, and Al-Hallaj. A comparison of lead acid to lithium-ion in stationary storage applications. 2012. Cited on page 88.
- Mikael Axin, Björn Eriksson, and Petter Krus. Flow versus pressure control of pumps in mobile hydraulic systems. 2014. URL <http://www.diva-portal.org/smash/get/diva2:710461/FULLTEXT01.pdf>. Cited on page 4.
- Berkner. How, why, and when to apply electric motors to mobile hydraulic systems. 2008. URL http://www.parkermotion.com/whitepages/applying_elec_motors_to_hydraulic_systems.pdf. Cited on pages 3 and 91.
- Burwell. Performance/cost comparison of induction-motor & permanent-magnet-motor in a hybrid electric car. 2013. URL <http://www.coppermotor.com/wp-content/uploads/2013/08/Techno-Frontier-2013-MBurwell-ICA-EV-Traction-Motor-Comparison-v1.8-Eng1.pdf>. Cited on pages 71 and 92.
- DiRenzo. Switched reluctance motor control – basic operation and example using the tms320f240. 2000. URL <http://www.ti.com/lit/an/spra420a/spra420a.pdf>. Cited on page 91.
- Encyclopaedia-Britannica. *Encyclopaedia Britannica Online Academic Edition*. Encyclopædia Britannica Inc, 2015. URL <http://www.britannica.com/EBchecked/topic/56126/battery>. Cited on page 88.

- EPA and Amarakoon et al. Application of life-cycle assessment to nanoscale technology: Lithium-ion batteries for electric vehicles. 2013. URL <http://www.epa.gov/dfe/pubs/projects/lbnp/final-li-ion-battery-lca-report.pdf>. Cited on page 89.
- Björn Eriksson. Mobile fluid power systems design. 2010. URL <http://www.diva-portal.org/smash/get/diva2:370276/FULLTEXT01.pdf>. Cited on page 4.
- Hansson. Miljontals människor drabbade av blyförgiftning på grund av illegal blyutvinning. 2014. Cited on page 88.
- Hashernnia and Asaei. Comparative study of using different electric motors in the electric vehicles. 2008. URL http://www.researchgate.net/profile/Mohammad_Naser_Hashemnia/publication/224394177_Comparative_study_of_using_different_electric_motors_in_the_electric_vehicles/links/00b7d529ef1b342acb000000.pdf. Cited on pages 91 and 92.
- Jonas Hällén. Här återvinns dina mobilbatterier. 2009. URL http://www.nyteknik.se/nyheter/energi_miljo/miljo/article263429.ece. Cited on page 78.
- INSG and Stewart. The global e-bike market. 2014. Cited on page 88.
- Jha. *Next-Generation Batteries and Fuel Cells for Commercial, Military, and Space Applications*. Taylor and Francis Group, 2012. Cited on page 88.
- Keyes and Eng. Electric motors energy efficiency reference guide. 2007. URL http://www.hydroone.com/MyBusiness/SaveEnergy/Documents/Electric_Motors_Reference_Guide.pdf. Cited on pages 91 and 92.
- Tianliang Lin, Qingfeng Wang, Baozan Hu, and Wen Gong. Development of hybrid powered hydraulic construction machinery. 2009. Cited on page 3.
- Linden and Reddy. Handbook of batteries - a short battery primer. 2006. Cited on page 88.
- Darko Lovrec, Mitja Kastrevc, and Samo Ulaga. Electro-hydraulic load sensing with a speed-controlled hydraulic supply system on forming-machines. 2008. Cited on page 4.
- Tatiana A. Minav, Lasse I.E. Laurila, and Juha J. Pyrhönen. Analysis of electro-hydraulic lifting system's energy efficiency with direct electric drive pump control. 2012. URL <http://www.sciencedirect.com.e.bibl.liu.se/science/article/pii/S092658051200204X>. Cited on page 4.
- Pierozynski. On the low temperature performance of nickel-metal hydride (nimh) batteries. 2011. Cited on page 88.

- Patrick Stegemann and Barun Acharya. Enabling intelligent and energy efficient hydraulic systems with electric pump controls. 2011. URL http://www.nfpa.com/events/pdf/2011_eehpc/03-nfpa-barun-final.pdf. Cited on page 4.
- Targray. *Li-ion Battery Materials*, 2014. URL <http://www.targray.com/li-ion-battery>. Cited on page 89.
- Tadej Tasner and Darko Lovrec. Maximum efficiency control – a new strategy to control electrohydraulic systems. 2014. Cited on page 3.
- Umans. *Fitzgerald & Kingsley*. McGraw-Hill, seventh edition, 2014. Cited on pages 27 and 30.
- USGS. Usgs minerals information. 2015. URL <http://minerals.usgs.gov/minerals/pubs/commodity>. Cited on page 89.



Upphovsrätt

Detta dokument hålls tillgängligt på Internet — eller dess framtida ersättare — under 25 år från publiceringsdatum under förutsättning att inga extraordinära omständigheter uppstår.

Tillgång till dokumentet innebär tillstånd för var och en att läsa, ladda ner, skriva ut enstaka kopior för enskilt bruk och att använda det oförändrat för icke-kommersiell forskning och för undervisning. Överföring av upphovsrätten vid en senare tidpunkt kan inte upphäva detta tillstånd. All annan användning av dokumentet kräver upphovsmannens medgivande. För att garantera äktheten, säkerheten och tillgängligheten finns det lösningar av teknisk och administrativ art.

Upphovsmannens ideella rätt innefattar rätt att bli nämnd som upphovsman i den omfattning som god sed kräver vid användning av dokumentet på ovan beskrivna sätt samt skydd mot att dokumentet ändras eller presenteras i sådan form eller i sådant sammanhang som är kränkande för upphovsmannens litterära eller konstnärliga anseende eller egenart.

För ytterligare information om Linköping University Electronic Press se förlagets hemsida <http://www.ep.liu.se/>

Copyright

The publishers will keep this document online on the Internet — or its possible replacement — for a period of 25 years from the date of publication barring exceptional circumstances.

The online availability of the document implies a permanent permission for anyone to read, to download, to print out single copies for his/her own use and to use it unchanged for any non-commercial research and educational purpose. Subsequent transfers of copyright cannot revoke this permission. All other uses of the document are conditional on the consent of the copyright owner. The publisher has taken technical and administrative measures to assure authenticity, security and accessibility.

According to intellectual property law the author has the right to be mentioned when his/her work is accessed as described above and to be protected against infringement.

For additional information about the Linköping University Electronic Press and its procedures for publication and for assurance of document integrity, please refer to its www home page: <http://www.ep.liu.se/>